Supporting Information

Manipulation of 1D and 2D Self-assembly via Geometry Modulation of Adamantane Isocyanide Pt(II) Complexes

*Fang Yang, Heyang Li, Huijie Li and Xiaoming He**

*To whom correspondence should be addressed

Key Laboratory of Applied Surface and Colloid Chemistry (Ministry of Education), School of Chemistry and Chemical Engineering, Shaanxi Normal University, Xi'an 710119, P.R. China

*Corresponding Author Email: xmhe@snnu.edu.cn

1. Experimental Section

1.1 Materials and Instruments. All chemical reagents were purchased from commercial sources (Aldrich, Alfa Aesar, Energy Chemical, and Adamas) and were used as received unless otherwise noted. (-)-4,5-Pinene-6'-phenyl-2,2'-bipyridine **(La)** and **Pt(La)Cl** were prepared according to reported procedures.[S1]

^{1}H NMR and ^{13}C NMR spectra were obtained on 400 MHz and 600 MHz BRUKER spectrometers. Mass spectrometry data were collected on a Bruker maxis UHR-TOF mass spectrometer in ESI positive mode. X-ray single crystal diffraction data were collected on a Nonius Kappa CCD diffractometer using Mo K*a* radiation (λ) 0.71073 Å (graphite monochromator). Ultraviolet-visible (UV-vis) absorption spectra were obtained on Cary 3500 spectrometer. Emission spectra and the absolute quantum yields were recorded on a Horiba FluoroMax Plus spectrofluorometer. CD experiments were performed using a Chirascan CD spectrometer. PL lifetimes were measured using an FLS1000 fluorescence spectrometer (Edinburgh) at room temperature. CPL spectra and subsequently derived glum values were recorded using an OLIS CPL Solo spectrofluorometer and the globalworks software suite. Scanning electron microscopy (SEM) was performed using a Hitachi SU8220 instrument. Transmission electron microscopy (TEM) was performed using a Hitachi TEM HT 7800 instrument operating at 80 kV acceleration voltage. Atomic force microscopy (AFM) experiments were performed on an Asylum Research Cypher VRS (Oxford instruments) atomic force microscope equipped with a Scan Asyst-HR fast scanning module and a Scan Asyst Air-HR probe (tip radius, 2 nm), utilizing peak force feedback control.

1.2 Synthesis

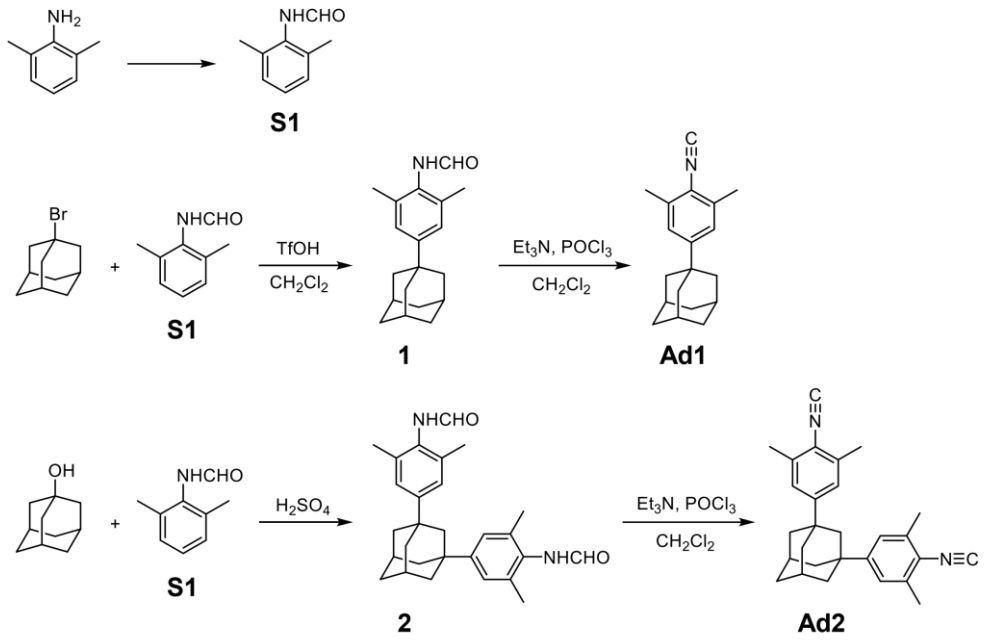

Scheme S1. Synthetic routes towards **Ad1** and **Ad2**.

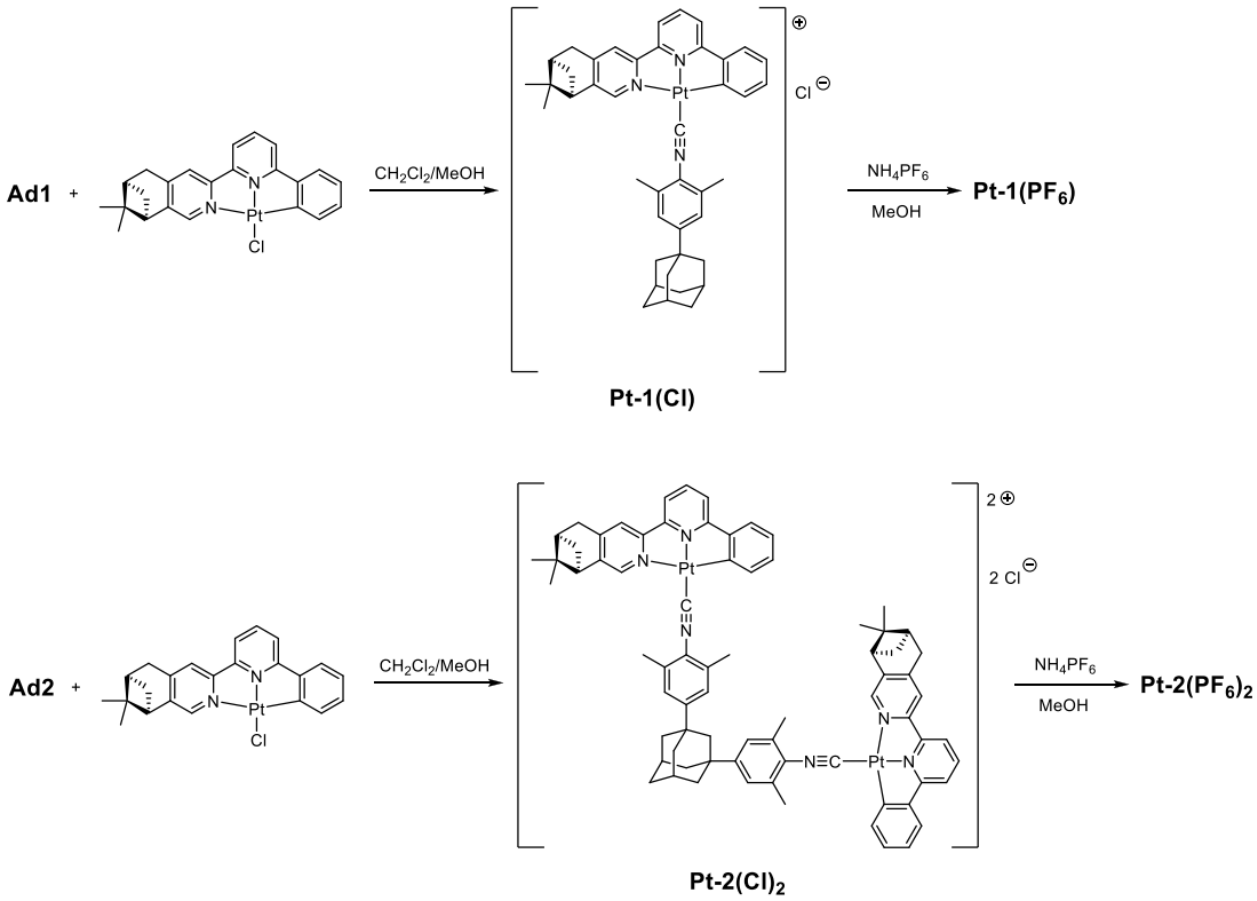

Scheme S2. Synthetic routes towards **Pt-1(PF$_6$)** and **Pt-2(PF$_6$)$_2$**.

Synthesis of 4-formylamino-3,5-dimethylbenzene (S1). A mixture of acetic anhydride (8.85 g, 86.65 mmol) and formic acid (7.80 g, 82.52 mmol) is heated with stirring for 2 h at 50-60 ℃ in a flask fitted with a drying tube. The solution is cooled to room temperature. 2,6-dimethylaniline (5.0 g, 41.26 mmol) dissolved in 100 mL dry CH_2Cl_2 is added gradually at 0 ℃. Then the mixture is stirred for 2 h at room temperature. After that, 100 mL n-hexane was added and a large number of white crystals was obtained. Yield: 4.0 g, 72 %. ^{1}H NMR (600 MHz, $CDCl_3$): δ/ppm = 8.43 (s, 1H), 8.10 (d, J = 12.0 Hz, 1.25H), 7.17-7.09 (m, 7H), 2.31 (s, 6H), 2.27 (s, 6H). The ^{1}H NMR spectrum matches well with reported data (*Angew. Chem. Int. Ed.* **2015**, *54*, 13332-13336).

Synthesis of 1-(3,5-dimethyl-4-formylaminophenyl) adamantane (1). To a solution of 4-formylamino-3,5-dimethylbenzene (2.1 g, 14.0 mmol) in dry CH_2Cl_2 (20 mL), was added 1-bromoadamantane (3.0 g, 14.0 mmol) and TfOH (8.4 g, 56.0 mmol) under N_2. The reaction mixture was stirred at 50 ℃ for 24 h. After cooling down to room temperature, the reaction mixture was poured into water (100 mL) and extracted several times with CH_2Cl_2. The combined organic layer was dried over $MgSO_4$, filtered and evaporated to get the desired product. This was directly used for further reaction without purification. HRMS: m/z calculated for $C_{19}H_{26}NO$ $[M+H]^+$, 284.2009, found, 284.2012.

Synthesis of 1-(3,5-dimethyl-4-phenylisocyanide) adamantane (Ad1). To a solution of 1-(3,5-dimethyl-4-formylaminophenyl) adamantane (3.0 g, 16.93 mmol; 1.0 eq) in dry CH_2Cl_2 (100 mL), was added Et_3N (3.43 g, 4.7 mL, 33.86 mmol; 2.0 eq) under N_2. The solution was cooled to 0 ℃ and $POCl_3$ (7.79 g, 4.73 mL, 50.29. mmol; 3.0 eq) was added to it dropwise. The reaction mixture was stirred at 0 ℃ for 2 h. Then it was quenched with saturated aqueous Na_2CO_3 solution and the resulting mixture was stirred for another 6 h. The organic part was extracted with CH_2Cl_2 and the combined organic

layer was washed with brine, dried over $MgSO_4$, filtered and concentrated under vacuum. The product was purified by column chromatography with silica gel eluting with PE/CH_2Cl_2 (10:1). Yield: 1.0 g, 36 %. ^{1}H NMR (600 MHz, $CDCl_3$): δ/ppm = 7.07 (s, 2H; C_6H_2), 2.41 (s, 6H; CH_3), 2.10 (s, 3H; CH), 1.87 (s, 6H; CH_2), 1.82 - 1.71 (m, 6H; CH_2). ^{13}C NMR (150 MHz, $CDCl_3$): δ/ppm = 167.06 , 151.05 , 134.52 , 124.43, 48.65, 41.94, 37.23, 35.61, 29.32, 19.18. HRMS: m/z calculated for $C_{19}H_{23}N$ $[M+H]^+$, 266.1903; found, 266.1908.

Synthesis of 1,3-Bis(3,5-dimethyl-4-formylaminophenyl) adamantane (2). 1-Adamantanol (2.0 g, 13.14 mmol) and 4-formylamino-3,5-dimethylbenzene **(S1)** (3.92 g, 26.27 mmol) were added to a 100 mL three-necked flask. Subsequently, concentrated sulfuric acid (20 mL) was added slowly through a funnel, followed by stirring for 8 hours at 25 °C. Afterwards, the mixture was poured in deionized water (100 mL). The white precipitate was collected by filtration, and the crude product was further purified by recrystallization using ethanol/water (1/3, v/v) to afford the desired product (4.4 g, 79 %). This was directly used for further reaction without purification. HRMS: *m/z* calculated for $C_{28}H_{34}N_2O_2Na$ $[M+Na]^+$ 453.2512, found 453.2515.

Synthesis of 1,3-Bis(3,5-dimethyl-4-phenylisocyanide) adamantane (Ad2). To a solution of 1,3-bis(3,5-dimethyl-4-formylaminophenyl) adamantane (4.3 g, 10.0 mmol; 1.0 eq) in dry CH_2Cl_2 (120 mL), was added Et_3N (4.1 g, 5.6 mL, 40.0 mmol; 4.0 eq) under N_2. The solution was cooled to 0 ℃ and $POCl_3$ (9.2 g, 5.6 mL, 60.0 mmol; 6.0 eq) was added to it dropwise. The reaction mixture was stirred at 0 ℃ for 2 h. Then it was quenched with saturated aqueous Na_2CO_3 solution and the resulting mixture was stirred for another 6 h. The organic part was extracted with CH_2Cl_2 and the combined organic layer was washed with brine, dried over $MgSO_4$, filtered and concentrated under vacuum. The product was purified by column chromatography with silica gel eluting with DCM/PE

(2:1). Yield: 2.8 g, 70 %. ^{1}H NMR (600 MHz, $CDCl_3$): δ/ppm = 7.09 (s, 4H; C_6H_2), 2.42 (s, 12H; CH_3), 2.33 (s, 2H; CH_2), 1.91 (s, 10H; CH_2), 1.78 (s, 2H; CH). ^{13}C NMR (150 MHz, $CDCl_3$): δ/ppm = 152.13, 134.88, 134.30, 128.62, 127.73, 124.42, 42.98, 36.66, 36.18, 28.83, 19.17, 18.90. HRMS: m/z calculated for $C_{28}H_{30}N_2$ $[M+H]^+$, 395.2482; found, 395.2480.

Synthesis of Pt-1(Cl). A mixture of Pt(L_a)Cl (55.6 mg, 0.1 mmol) and **Ad1** (26.5 mg, 0.1 mmol) in CH_2Cl_2/MeOH (2:1, v/v; 6 mL) was stirred at room temperature for 6 h. The product was precipitated out by adding diethyl ether, collected by filtration, washed with diethyl ether and finally dried under vacuum. Yield: 96%. ^{1}H NMR (600 MHz, $CDCl_3$) δ/ppm = 9.39 (d, J = 9.4 Hz, 1H), 9.15 (d, J = 8.4 Hz, 1H), 8.29 (d, J = 3.7 Hz, 1H), 8.12 (d, J = 9.0 Hz, 1H), 7.68 (d, J = 8.0 Hz, 1H), 7.49 (d, J = 7.4 Hz, 1H), 7.39 (d, J = 7.4 Hz, 1H), 7.28 (s, 1H), 7.24 (s, 1H), 7.17 (d, J = 26.7 Hz, 2H), 3.49 – 3.33 (m, 3H), 2.80 (dd, J = 24.1, 5.7 Hz, 2H), 2.59 (d, J = 9.8 Hz, 5H), 2.40 (s, 1H), 2.14 (s, 2H), 1.91 (d, J = 2.8 Hz, 3H), 1.80 (d, J = 28.3 Hz, 4H), 1.43 (s, 3H), 1.26 (s, 5H), 0.70 (s, 3H). ^{13}C NMR (150 MHz, $CDCl_3$): δ/ppm = 164.26, 155.82, 154.99, 153.87, 151.59, 148.99,147.19, 138.25, 135.87, 135.41, 132.48, 130.76, 128.84, 125.48, 124.82, 120.57, 120.47, 44.22, 42.71, 38.92, 36.51, 33.57, 31.01, 28.68, 25.84, 21.63, 19.17, 18.95. HRMS: m/z calculated for $C_{42}H_{44}N_3Pt$ $[M]^+$, 785.3181; found, 785.3185.

Synthesis of Pt-1(PF_6). To a solution of NH_4PF_6 (400 mg, 2.4 mmol) in MeOH (25 mL), was added methanol solution of **Pt-1(Cl)** (100 mg, 0.12 mmol). After stirring at room temperature for 12 h, the product was collected by centrifugation, washed with MeOH twice, and finally dried under vacuum. Yield: 93 %. ^{1}H NMR (600 MHz, d6-DMSO) δ/ppm = 8.61 (d, J = 17.7 Hz, 1H), 8.43 (d, J = 10.2 Hz, 1H), 8.24 (p, J = 7.1, 6.6 Hz, 2H), 8.10 (dd, J = 11.5, 7.4 Hz, 1H), 7.79 – 7.70 (m, 1H), 7.42 (dd, J = 50.4, 7.8 Hz, 3H), 7.18 (dt, J = 16.9, 7.8 Hz, 2H), 3.27 – 3.09 (m, 2H), 3.03 (q, J = 5.5 Hz,

1H), 2.78 (dt, *J* = 10.2, 5.3 Hz, 1H), 2.53 (s, 5H), 2.36 (s, 1H), 2.09 (s, 2H), 1.90 (s, 3H), 1.83 – 1.73 (m, 3H), 1.41 (s, 3H), 1.22 (d, *J* = 9.9 Hz, 2H), 0.64 (d, *J* = 4.0 Hz, 3H). ^{13}C NMR (150 MHz, d6-DMSO): *δ*/ppm = 164.16, 155.71, 153.87, 151.52, 148.78, 147.17, 143.73, 138.26, 137.34, 135.86, 135.39, 132.46, 130.76, 128.84, 126.37, 125.48, 124.83, 123.99, 120.49, 44.22, 42.71, 39.39, 38.92, 33.57, 31.01, 28.68, 25.83 , 21.62, 19.17, 18.95. ^{31}P NMR (600 MHz, d6-DMSO) *δ*/ppm = -144.2 (quint). HRMS: m/z calculated for $C_{42}H_{44}N_3Pt$ $[M]^+$, 785.3181; found, 785.3188.

Synthesis of Pt-2(Cl)$_2$. A mixture of **Pt(L$_a$)Cl** (55.6 mg, 0.1 mmol) and **Ad2** (19.7 mg, 0.05 mmol) in CH_2Cl_2/MeOH (2:1, v/v; 6 mL) was stirred at room temperature for 6 h. The product was precipitated out by adding diethyl ether, collected by filtration, washed with diethyl ether and finally dried under vacuum. Yield: 97%. ^{1}H NMR (600 MHz, d6-DMSO) *δ*/ppm = 8.55 (s, 2H), 8.42 (s, 2H), 8.23 (d, *J* = 12.1 Hz, 4H), 8.07 (d, *J* = 7.7 Hz, 2H), 7.70 (d, *J* = 7.8 Hz, 2H), 7.46 (s, 4H), 7.36 (d, *J* = 7.9 Hz, 2H), 7.16 (d, *J* = 25.5 Hz, 4H), 3.26 – 3.10 (m, 5H), 3.00 (s, 2H), 2.79 (d, *J* = 4.2 Hz, 2H), 2.53 (s, 13H), 2.35 (d, *J* = 24.5 Hz, 5H), 2.05 (s, 2H), 1.95 (s, 7H), 1.80 (s, 2H), 1.41 (s, 6H), 1.23 (s, 8H), 0.64 (s, 6H). HRMS: m/z calculated for $C_{74}H_{72}N_6Pt_2$ $[M]^{2+}$, 717.2550; found, 717.2538.

Synthesis of Pt-2(PF$_6$)$_2$. To a solution of NH_4PF_6 (432 mg, 2.65 mmol) in MeOH (25 mL), was added methanol solution of **Pt-2(Cl)$_2$** (100 mg, 0.066 mmol). The reaction was heated to 50 ºC for 2h. After that, the reaction was stirred at room temperature for 12 h. The product was collected by centrifugation, washed with MeOH twice, and finally dried under vacuum. Yield: 96 %. ^{1}H NMR (600 MHz, d6-DMSO) *δ*/ppm = 8.53 (s, 2H), 8.39 (s, 2H), 8.22 (dt, *J* = 17.6, 7.9 Hz, 4H), 8.06 (d, *J* = 7.7 Hz, 2H), 7.69 (d, *J* = 7.5 Hz, 2H), 7.45 (s, 4H), 7.36 (d, *J* = 6.9 Hz, 2H), 7.16 (dt, *J* = 25.6, 7.8 Hz, 4H), 3.25 – 3.10 (m, 5H), 2.99 (s, 2H), 2.78 (s, 3H), 2.34 (d, *J* = 28.0 Hz, 4H), 2.04 (s, 2H), 1.95 (s, 7H), 1.80 (s, 2H), 1.41 (s, 5H), 1.30 – 1.15 (m, 6H), 0.64 (s, 5H). ^{13}C NMR (150 MHz, d6-DMSO):

δ/ppm = 164.27, 155.81, 155.00, 151.60, 149.02, 148.79, 147.27, 145.65, 143.82, 138.16, 132.48, 126.76, 126.49, 126.36, 120.55, 120.46, 62.52, 44.22, 40.54, 39.39, 38.94, 33.58, 31.00, 25.83, 21.64, 19.01. ^{31}P NMR (600 MHz, d6-DMSO) δ/ppm = -144.2 (quint). HRMS: m/z calculated for $C_{74}H_{72}N_6Pt_2$ $[M]^{2+}$, 717.2550; found, 717.2547.

1.3 X-ray Crystals

Colorless needle-like crystals of **Ad1** and cubic-shaped crystals of **Ad2** can be obtained by slow evaporation of their saturated acetone solutions. The crystal data and structure refinement details are summarized in Table S1.

2. Supplementary Tables and Figures.

Table S1. Crystal data and structure refinement for **Ad1** and **Ad2.**

Compounds	**Ad1**	**Ad2**
Empirical formula	$C_{19}H_{23}N$	$C_{28}H_{30}N_2$
Formula weight	265.38	394.54
Temperature/K	200.00	153.00
Crystal system	Orthorhomic	Monoclinic
Space group	Pnma	$P2_1/c$
a/Å	11.2368(3)	6.7908(4)
b/Å	7.0029(2)	19.6373(13)
c/Å	19.2578(5)	16.4833(11)
α/°	90	90
β/°	90	90.029(3)
γ/°	90	90
Volume/ $Å^3$	1515.40(7)	2198.1(2)
Z	4	4
ρ_{calc} g/cm^3	1.163	1.198
μ / mm^{-1}	0.501	0.525
F(000)	576.0	856.0
Crystal size/ mm^3	0.3 × 0.2 × 0.12	0.5 × 0.3 × 0.1
Radiation	CuKα (λ = 1.54178)	CuKα (λ = 1.54178)
2θ range for data collection/°	9.112 to 136.18	7.002 to 136.678
Index ranges	$-13 \leq h \leq 13$, $-8 \leq k \leq 8$, $-18 \leq l \leq 23$	$-8 \leq h \leq 8$, $-23 \leq k \leq 22$, $-19 \leq l \leq 19$
Reflections collected	19743	31114
Independent reflections	1496 [R_{int} = 0.0419, R_{sigma} = 0.0189]	4009 [R_{int} = 0.0579, R_{sigma} = 0.0289]
Data / restraints / parameters	1496 / 0/ 114	4009 / 0/ 275
Goodness-of-fit on F^2	1.063	1.054
Final R indexes [I > 2σ(I)]	R_1 = 0.0481, wR_2 = 0.1251	R_1 = 0.0429, wR_2 = 0.1117
Final R indexes (all data)	R_1 = 0.0509, wR_2 = 0.1279	R_1 = 0.0562, wR_2 = 0.1195
Largest diff. peak and hole/ $eÅ^{-3}$	0.19 and -0.18	0.24 and -0.21
CCDC	2356079	2356080

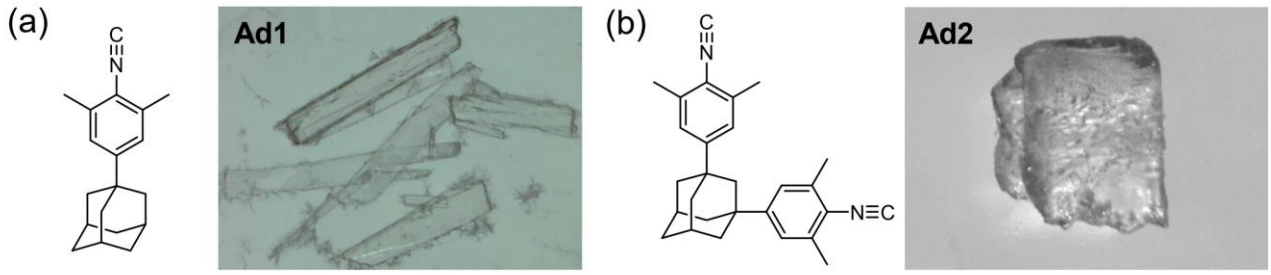

Figure S1. Molecular structures and single crystal pictures of (a) **Ad1** and (b) **Ad2**.

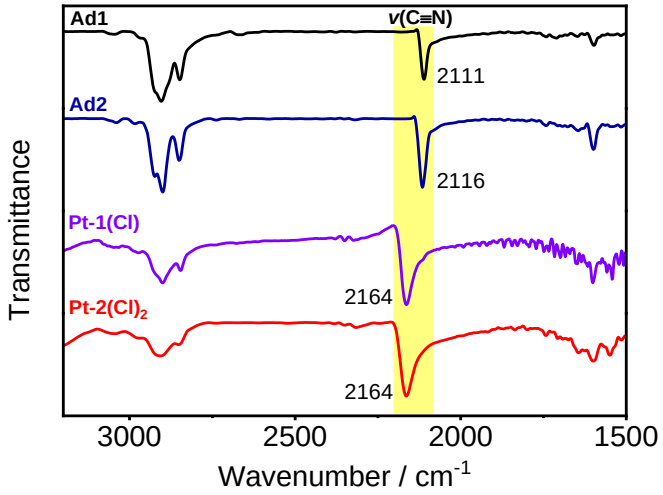

Figure S2. IR spectra of **Pt-1(Cl)**, **Pt-2(Cl)$_2$** and their corresponding isocyanides (**Ad1** and **Ad2**).

Additional discussion: Strong band due to ν(N≡C) was observed at 2164 cm^{-1} in the IR spectrum for complexes **Pt-1(Cl)** and **Pt-2(Cl)$_2$**, which is at a higher frequency than that found in the corresponding isocyanide ligands **Ad1** and **Ad2** at *ca.* 2110 cm^{-1}, confirming the successful synthesis of the complexes.

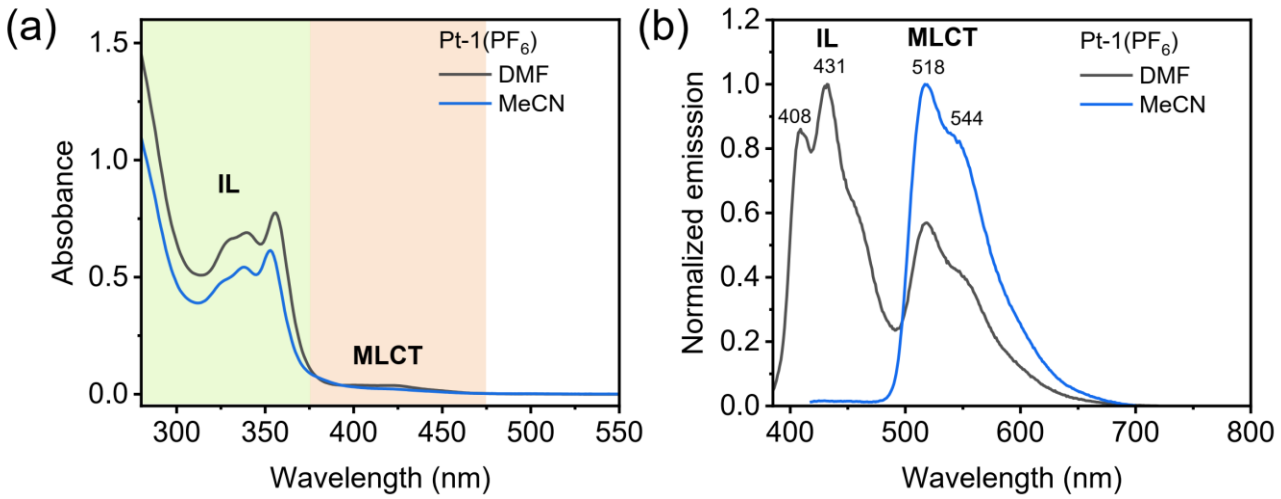

Figure S3. (a) UV-vis and (b) emission spectra of **Pt-1(PF$_6$)** in DMF and CH_3CN ($c = 4.0 \times 10^{-5}$ M) at 298 K.

Additional discussion: The high-energy absorption band at *ca.* 300-375 nm is assigned to the intra-ligand (IL) [π→π*] transitions of C^N^N pincer ligand, while the low-energy absorption band at ca. 375-475 nm is assigned to metal-to-ligand charge transfer (MLCT). The emission profiles of **Pt-1(PF$_6$)** in DMF and CH_3CN are different, which is tentatively attributed to the solvent polarity. In DMF, both IL and MLCT excited states can be observed; while its CH_3CN solution only display MLCT emission.

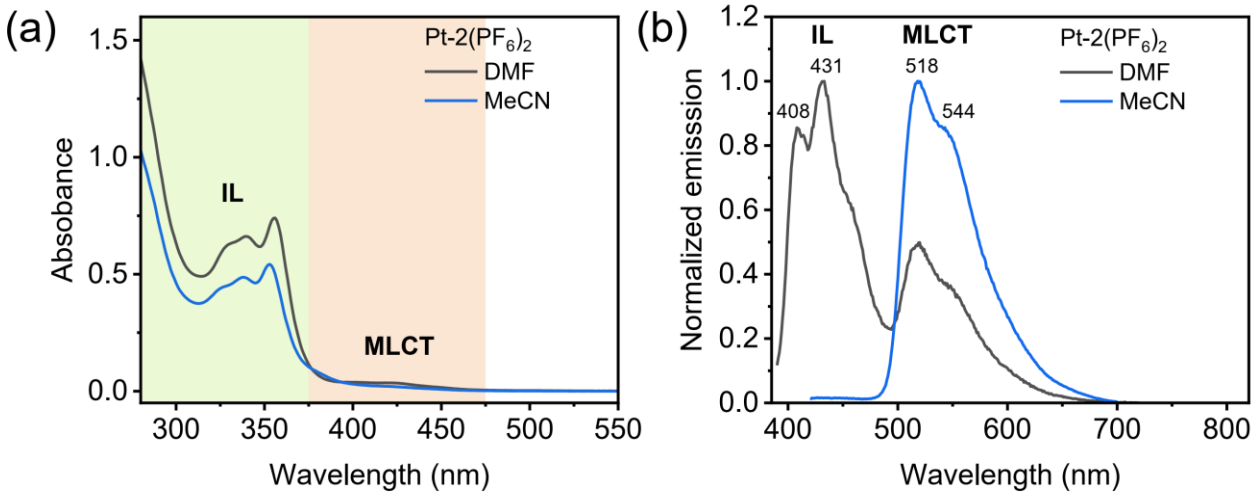

Figure S4. (a) UV-vis and (b) emission spectra of **Pt-2(PF$_6$)$_2$** in DMF and CH_3CN (c = 2.0 × 10^{-5} M) at 298 K.

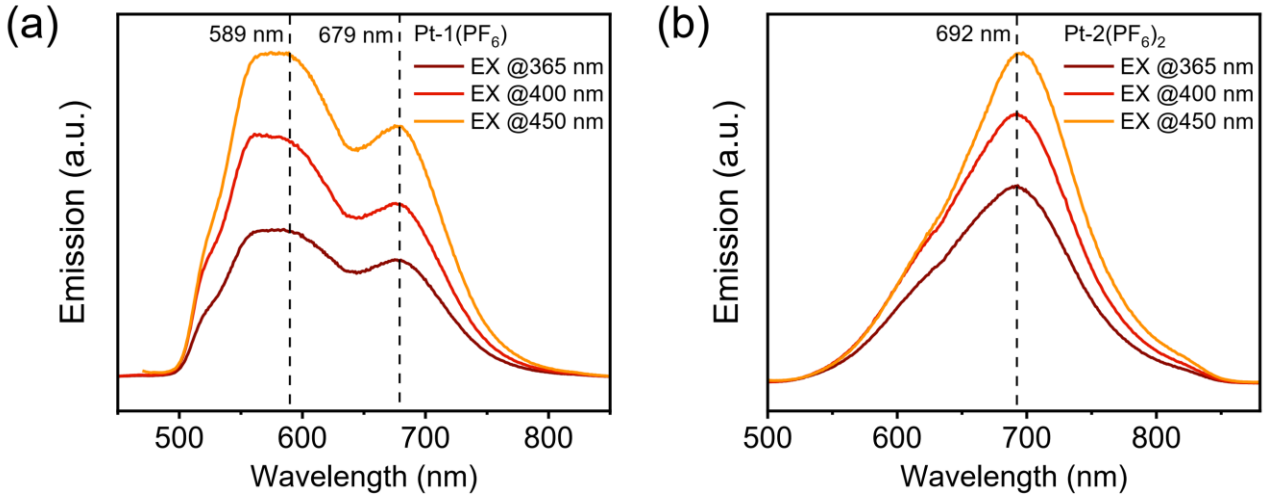

Figure S5. Emission spectra of (a) **Pt-1(PF$_6$)** and (b) **Pt-2(PF$_6$)$_2$** in solid-states at 298 K.

Additional discussion: The appearance of two emission peaks for **Pt-1(PF$_6$)** in the solid state probably results from the polymorphism involving different intermolecular interactions.

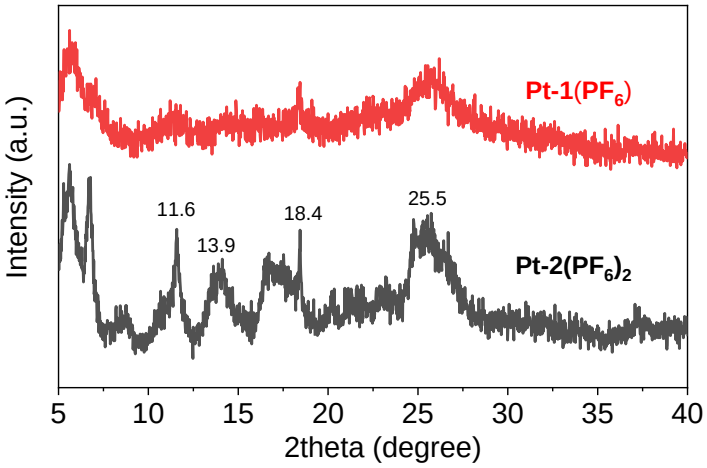

Figure S6. PXRD patterns of **Pt-1(PF$_6$)** and **Pt-2(PF$_6$)$_2$** in solid states.

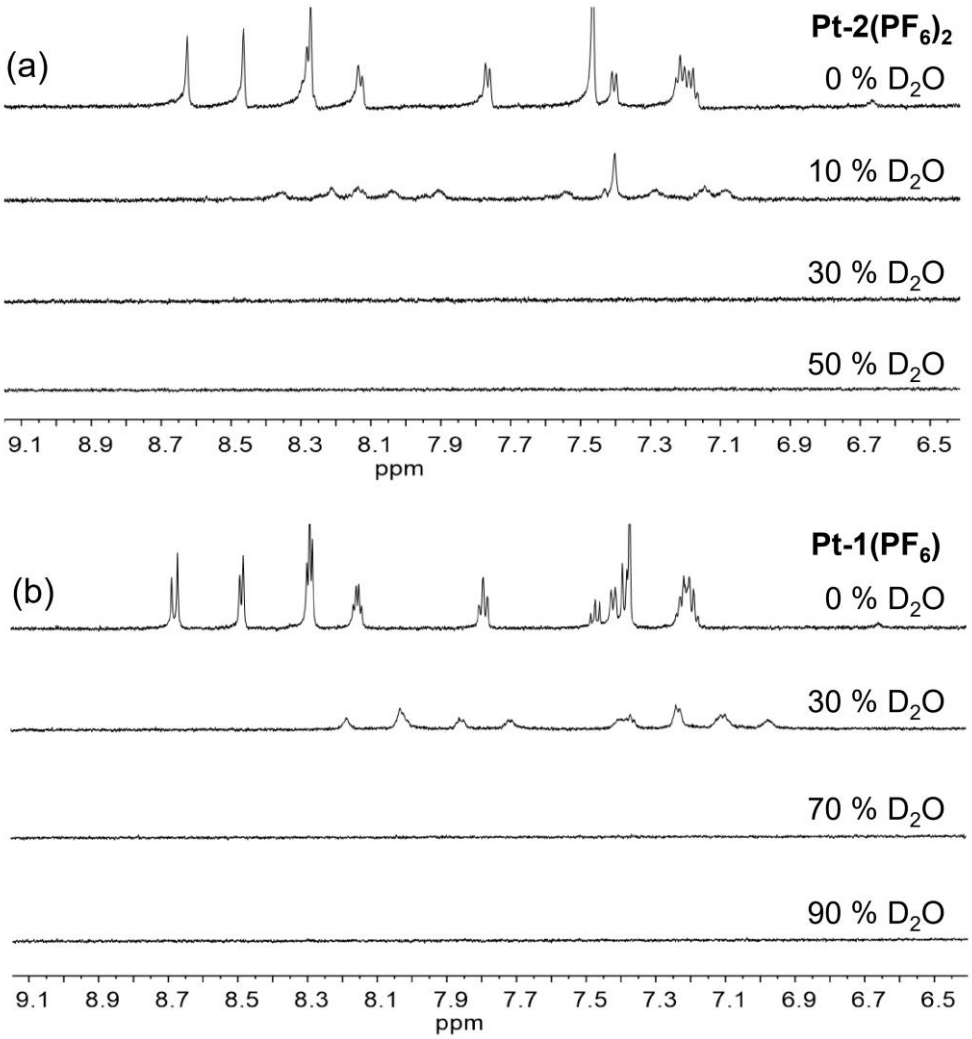

Figure S7. ^{1}H NMR spectral changes of (a) **Pt-2(PF$_6$)$_2$** (c = 1 mM) and (b) **Pt-1(PF$_6$)** (c = 2 mM) at different compositions of D_2O in d6-DMSO (600 MHz, 298 K).

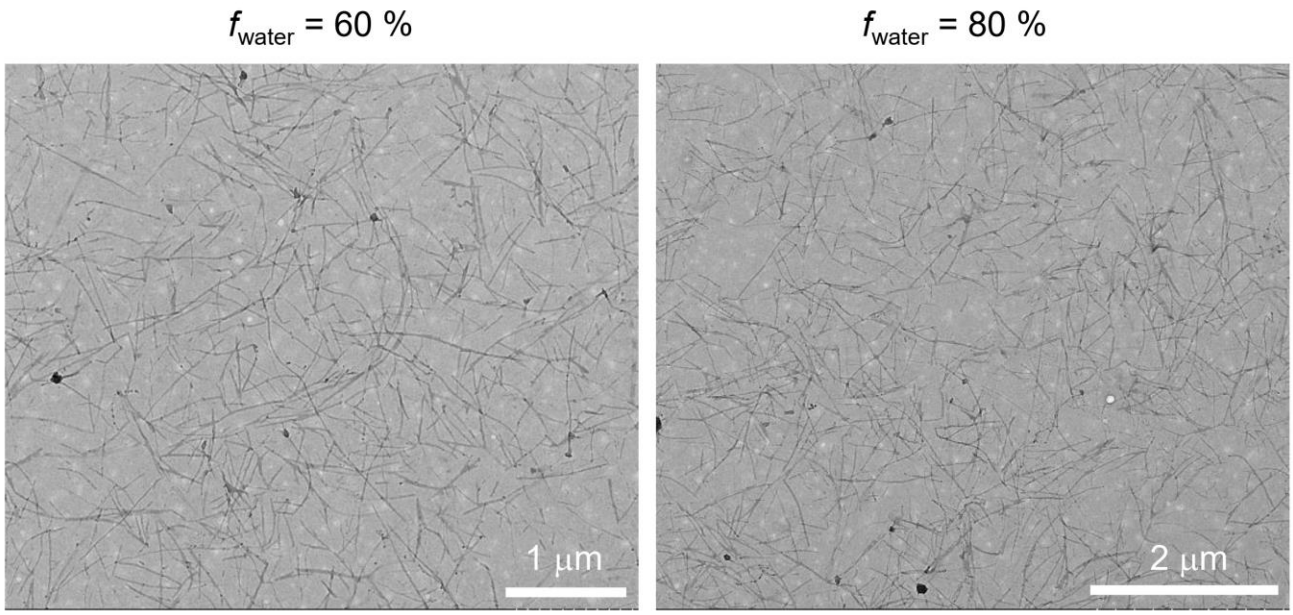

Figure S8. TEM images of **Pt-1(PF$_6$)** in H_2O-DMF mixtures with water fraction (f_{water}) of 60 % (left) and 80 % (right).

No visible morphology transformation was observed for **Pt-1(PF$_6$)** upon increasing f_{water} from 60% to 80%.

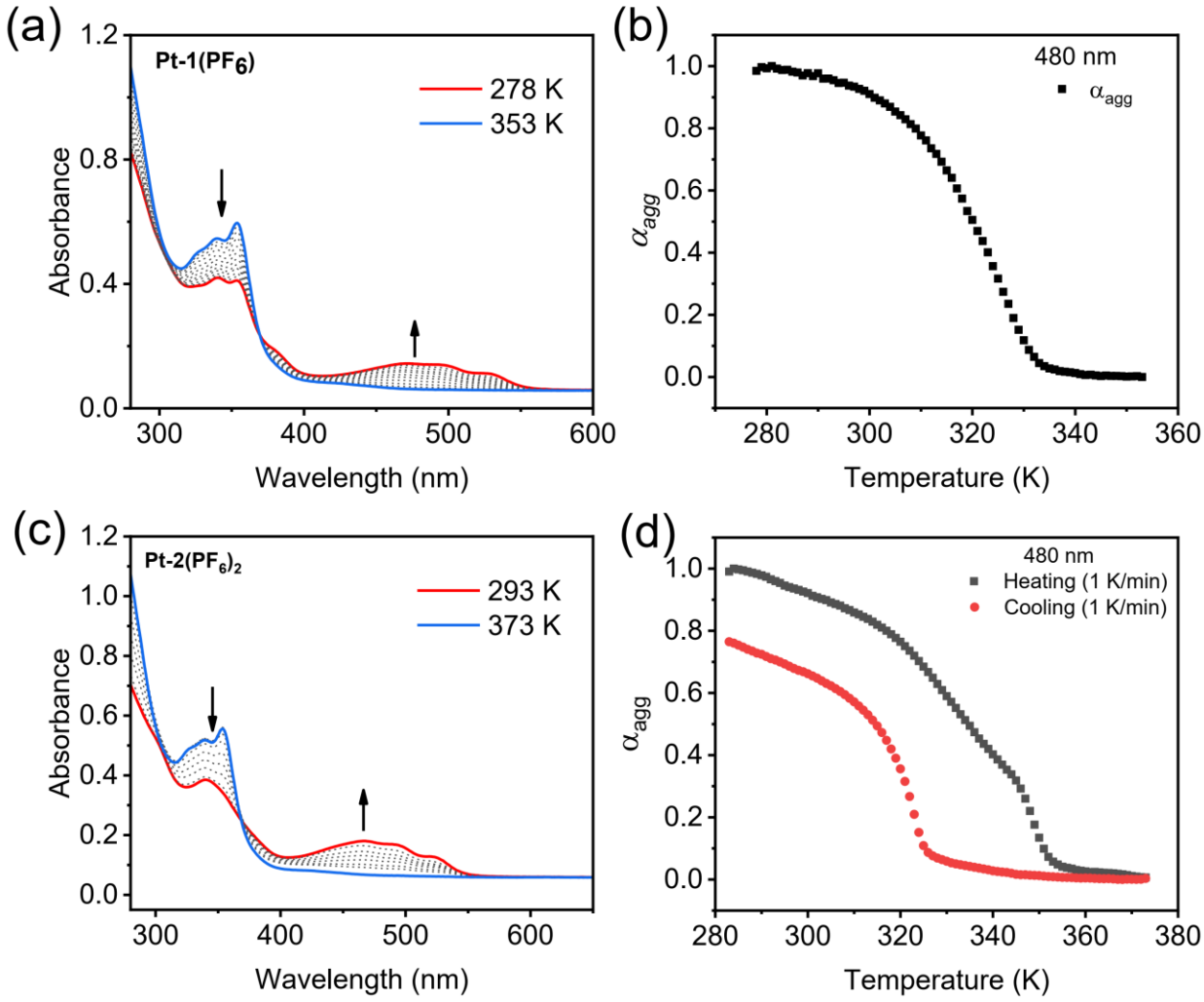

Figure S9. UV-vis absorption spectra traces on cooling a solution of (a) **Pt-1(PF$_6$)** (c = 4.0 × 10^{-5} M**)** in H_2O-DMF (6:4, v/v) and (c) **Pt-2(PF$_6$)$_2$** (c = 2.0 × 10^{-5} M**)** in H_2O-DMF (5:5, v/v) at a cooling rate of 1 K min^{-1}. (b, d) Degree of aggregation α_{agg} at 480 nm as a function of temperature. The red lines denote the mathematical model fitting of the curves.

Characterization (NMR and MS)

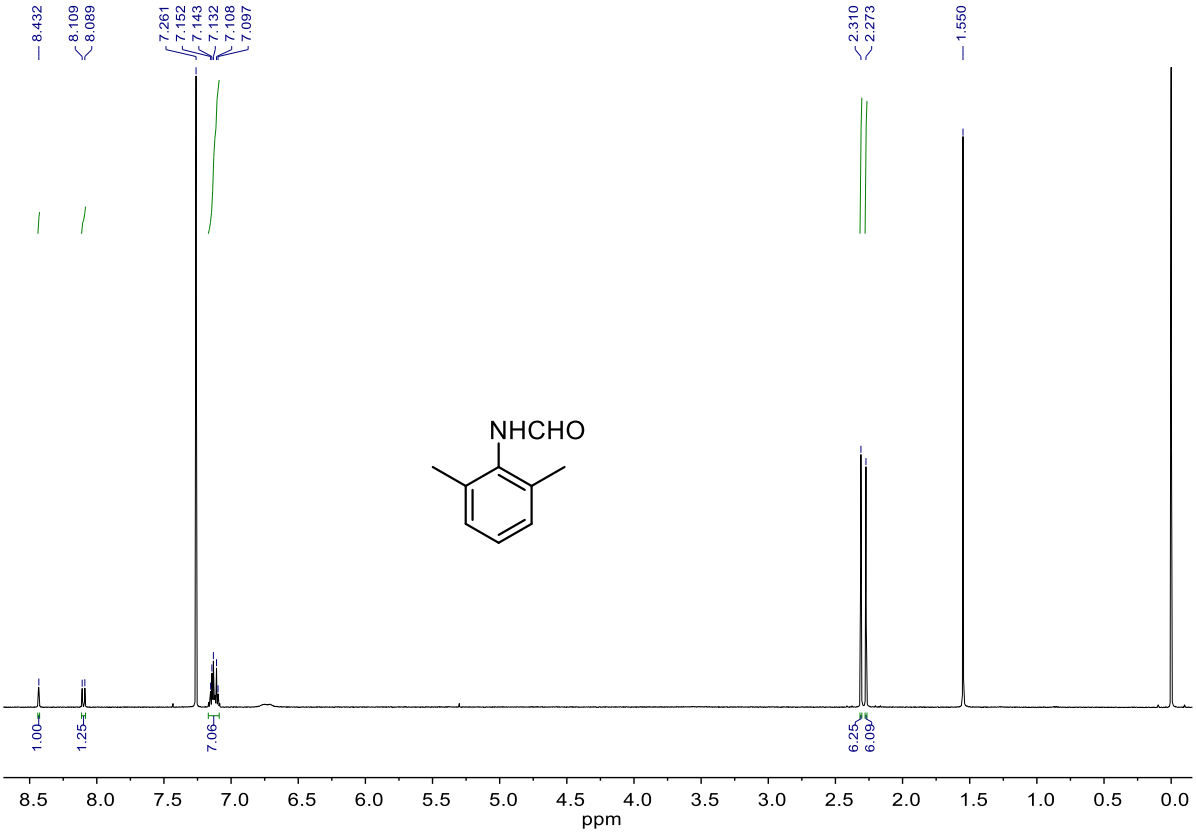

Figure S10. ^{1}H NMR spectrum of 4-formylamino-3,5-dimethylbenzene **(S1).**

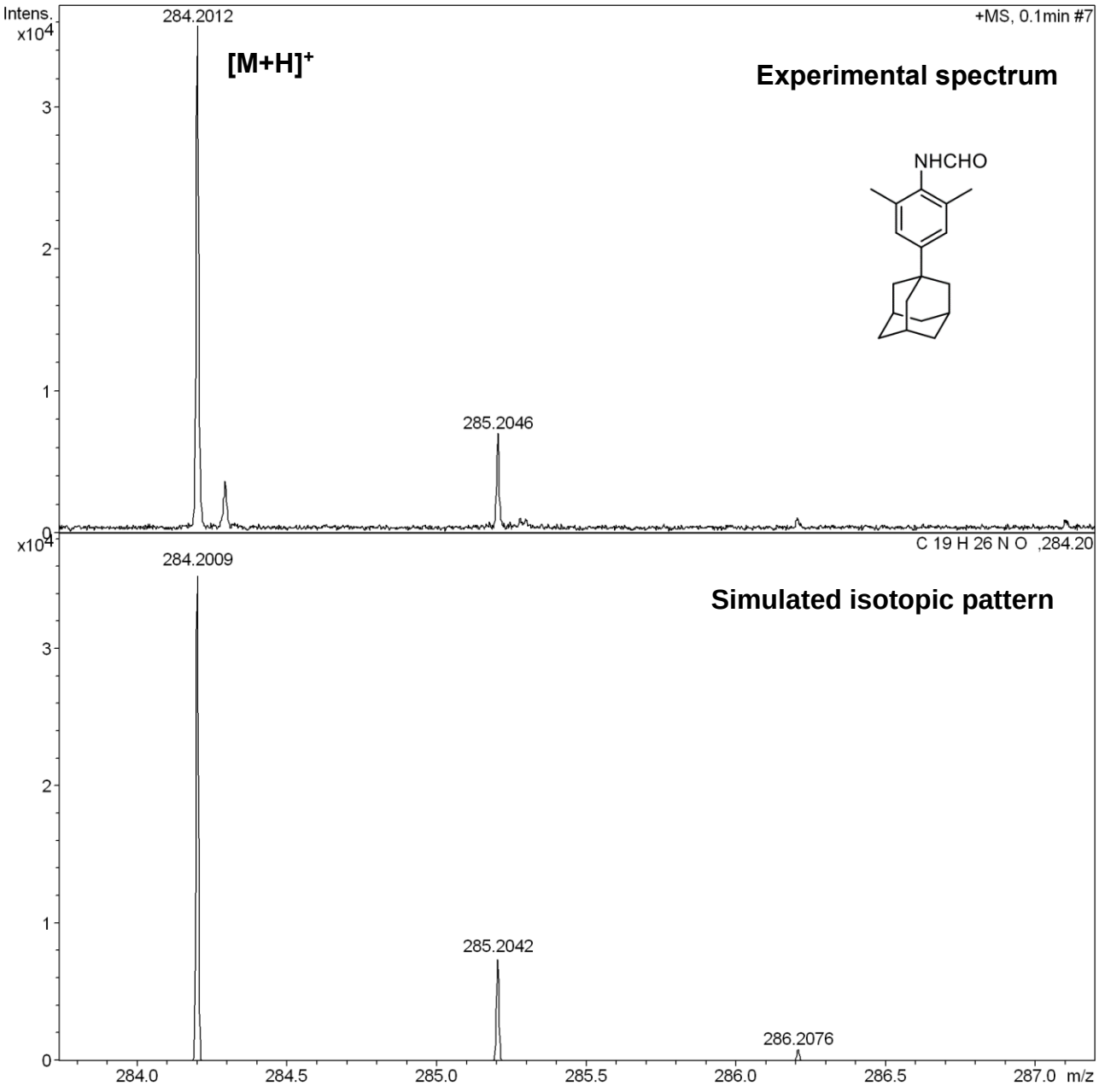

Figure S11. Mass spectrum of **1**.

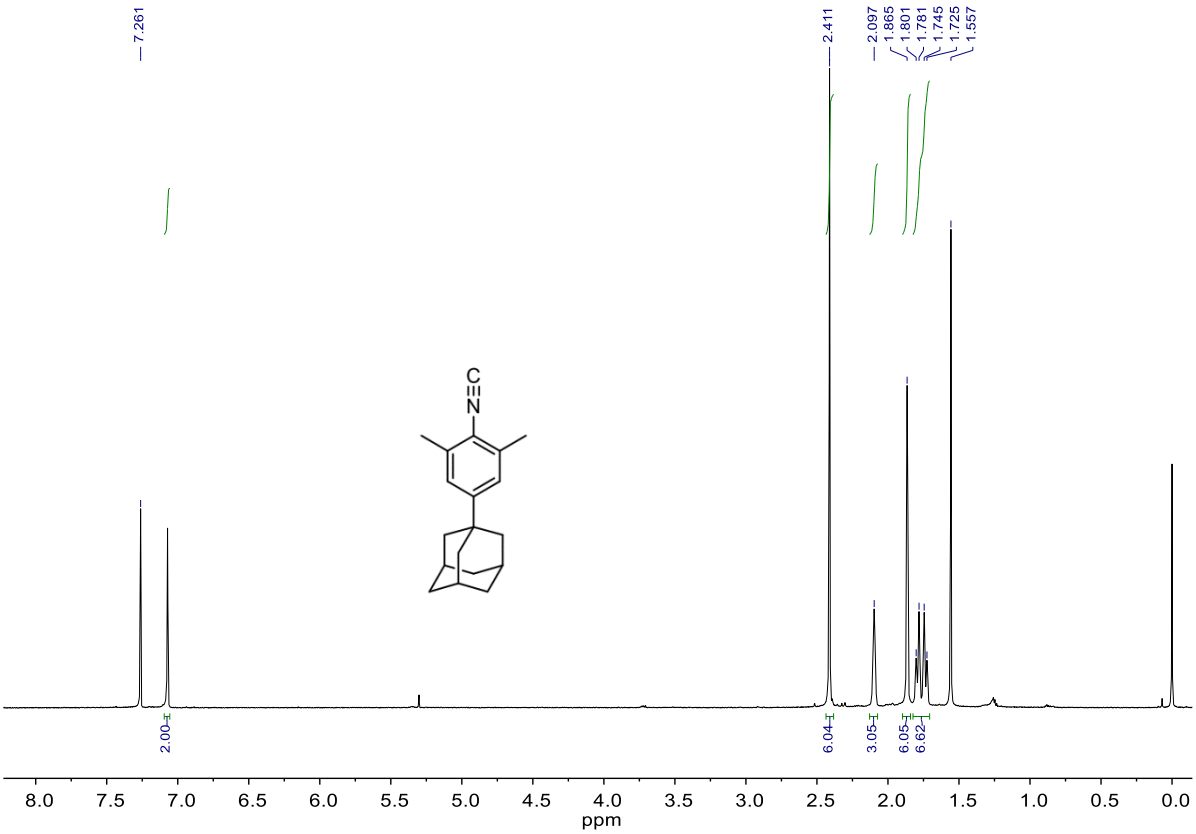

Figure S12. ^{1}H NMR spectrum of **Ad1** in $CDCl_3$.

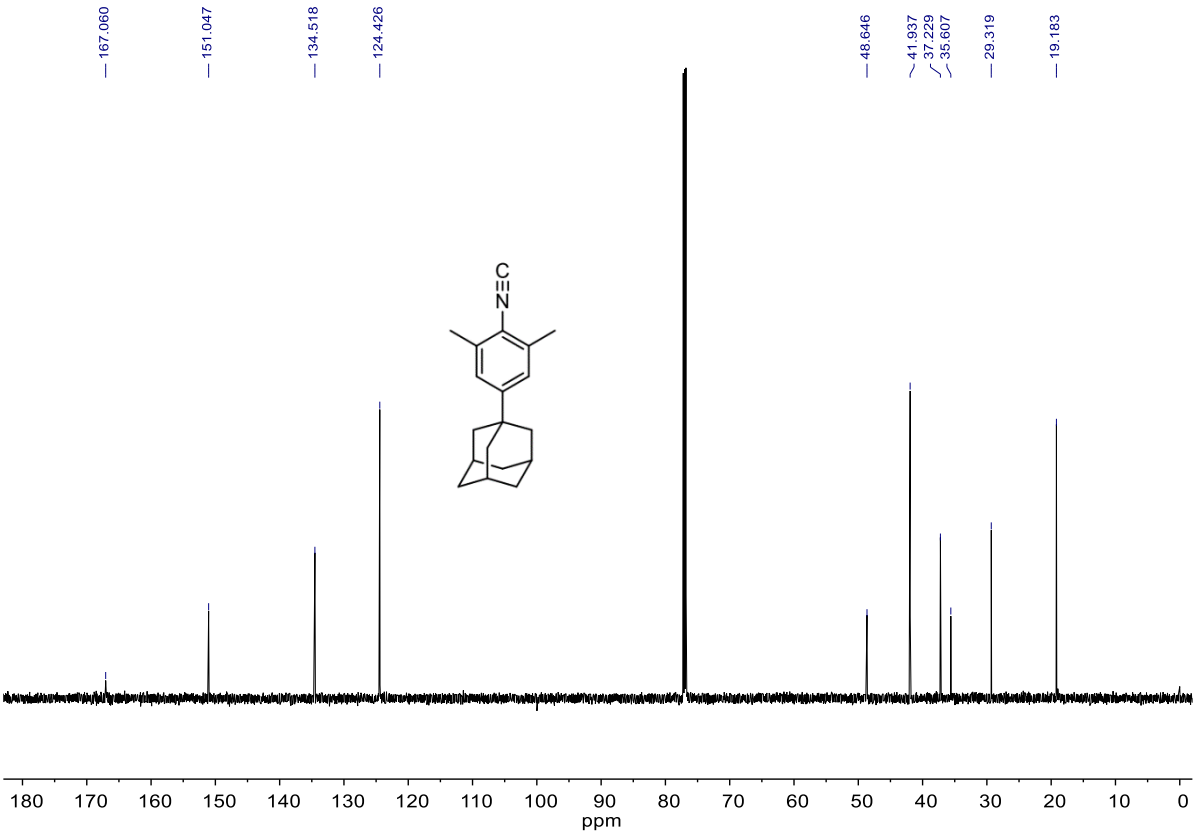

Figure S13. ^{13}C NMR spectrum of **Ad1** in $CDCl_3$.

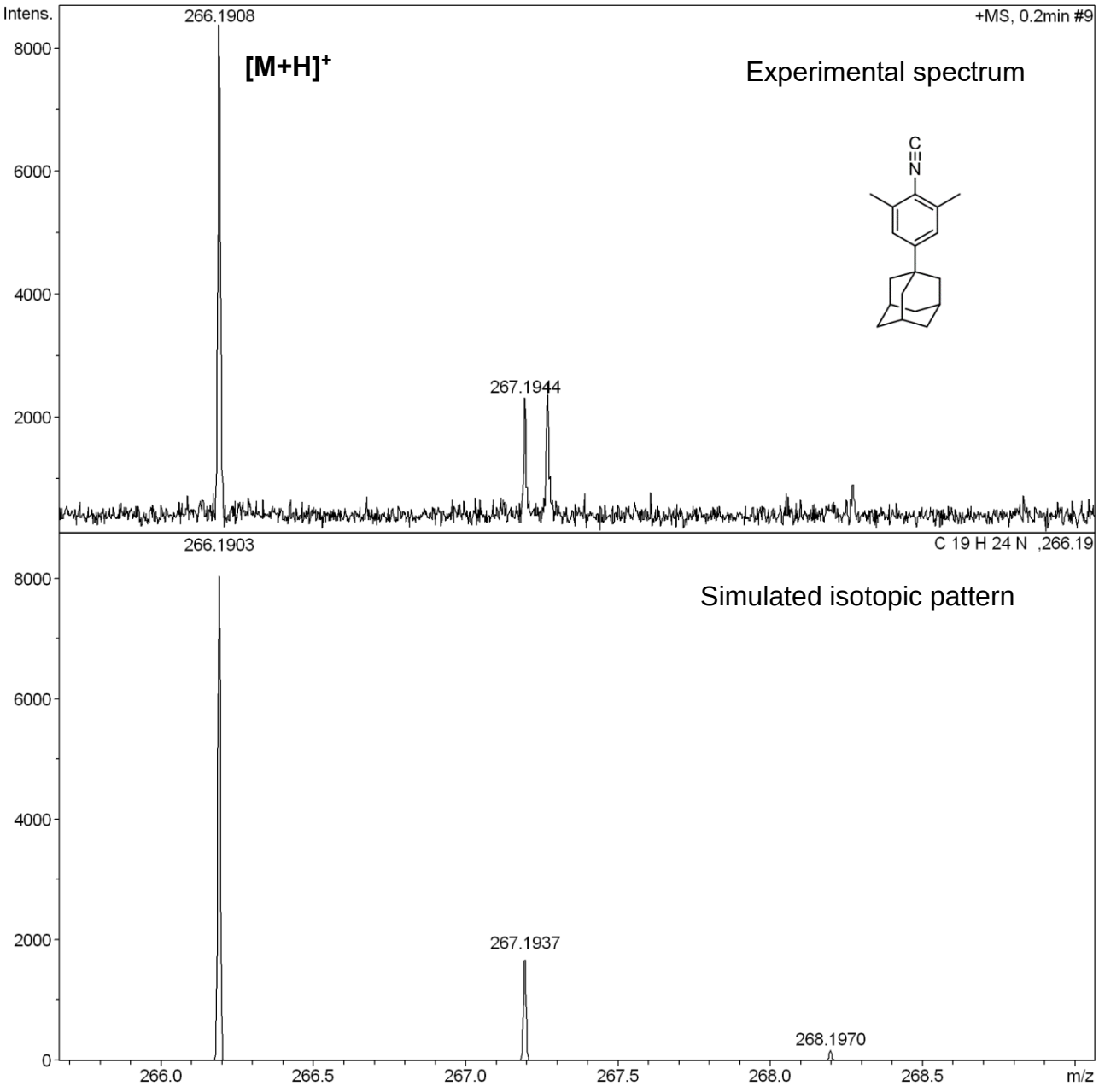

Figure S14. Mass spectrum of **Ad1**.

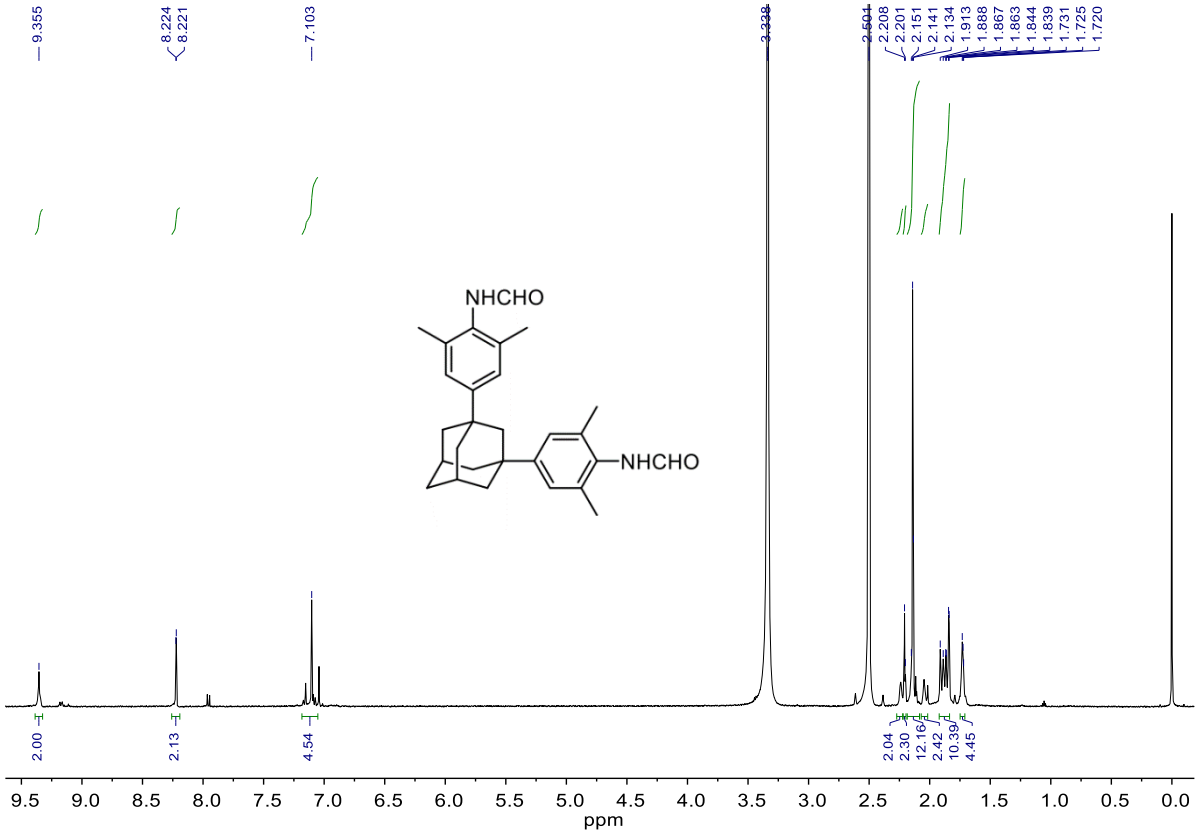

Figure S15. ^{1}H NMR spectrum of **2** in d6-DMSO.

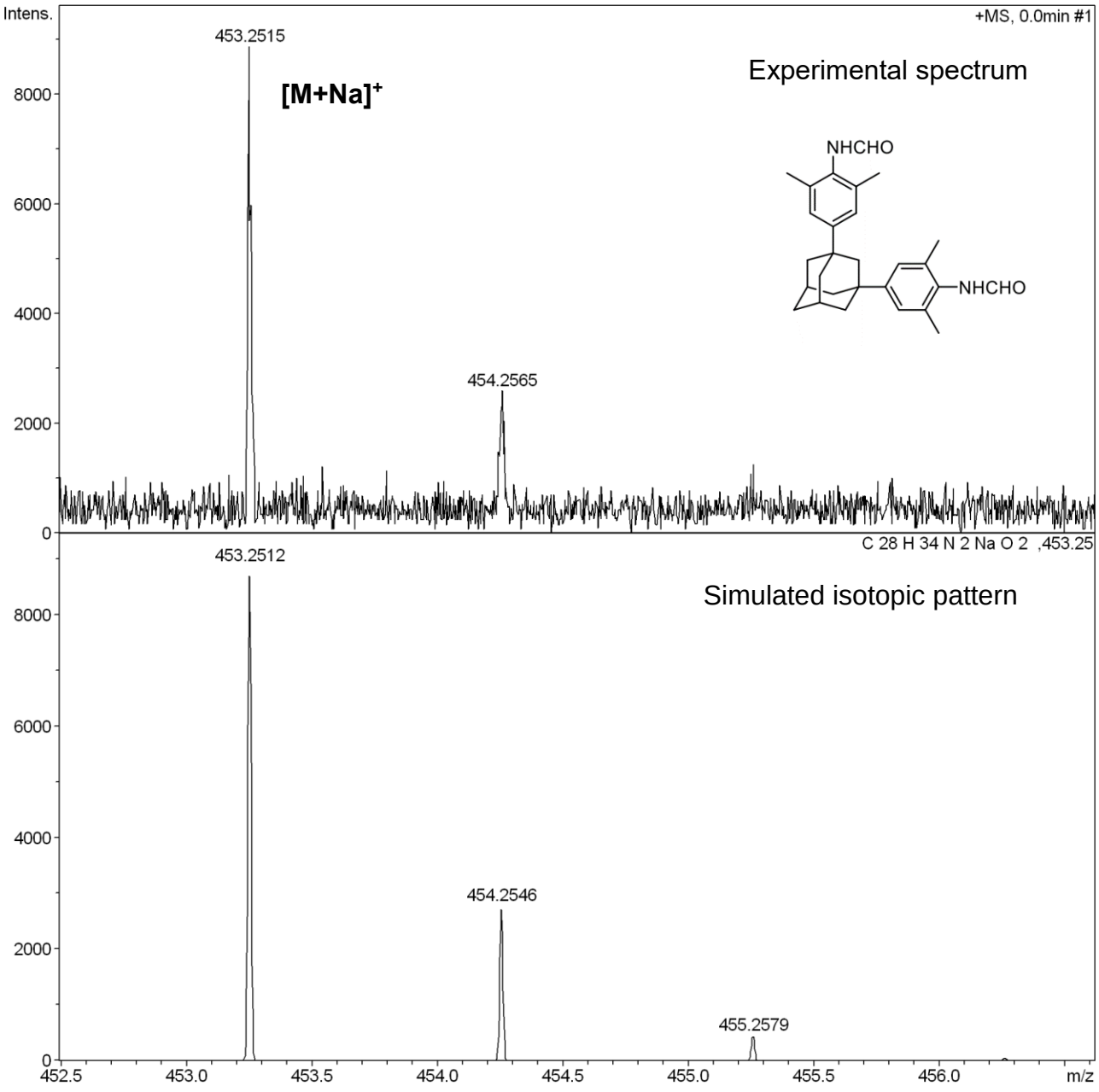

Figure S16. Mass spectrum of **2**.

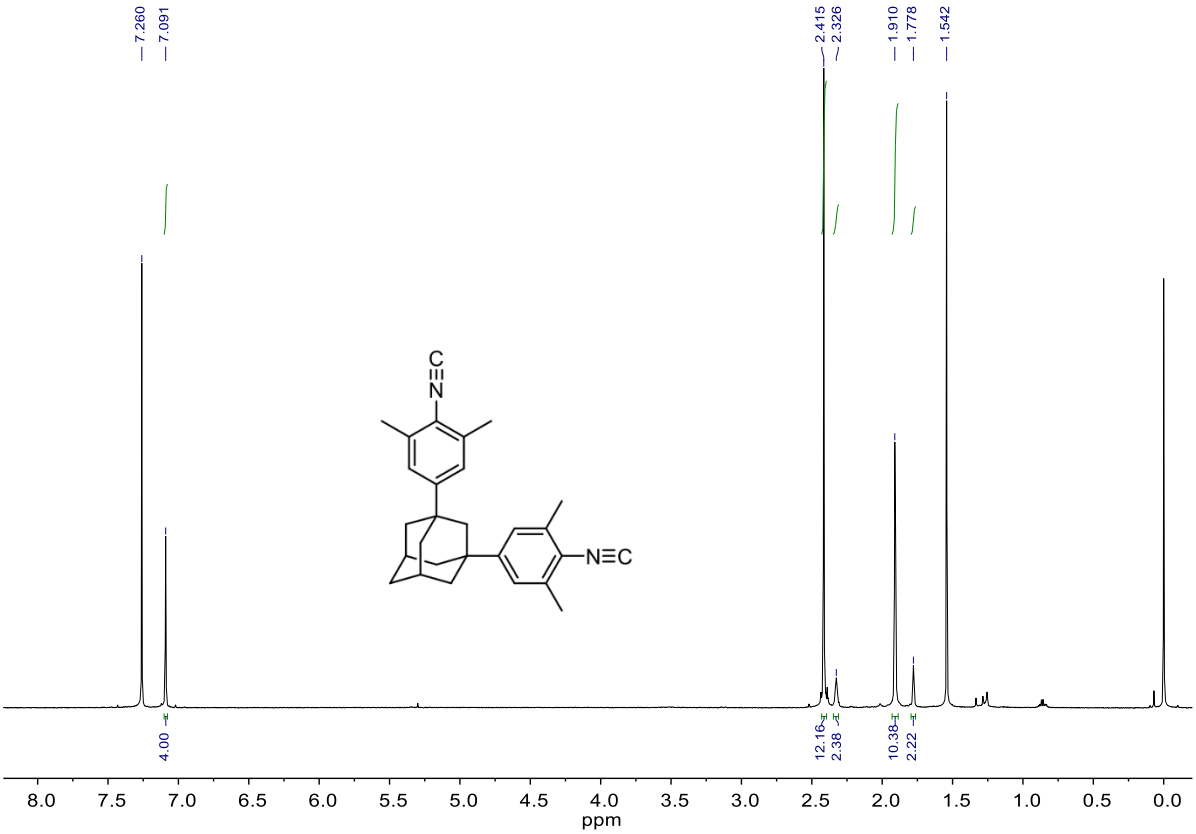

Figure S17. ^{1}H NMR spectrum of **Ad2** in $CDCl_3$.

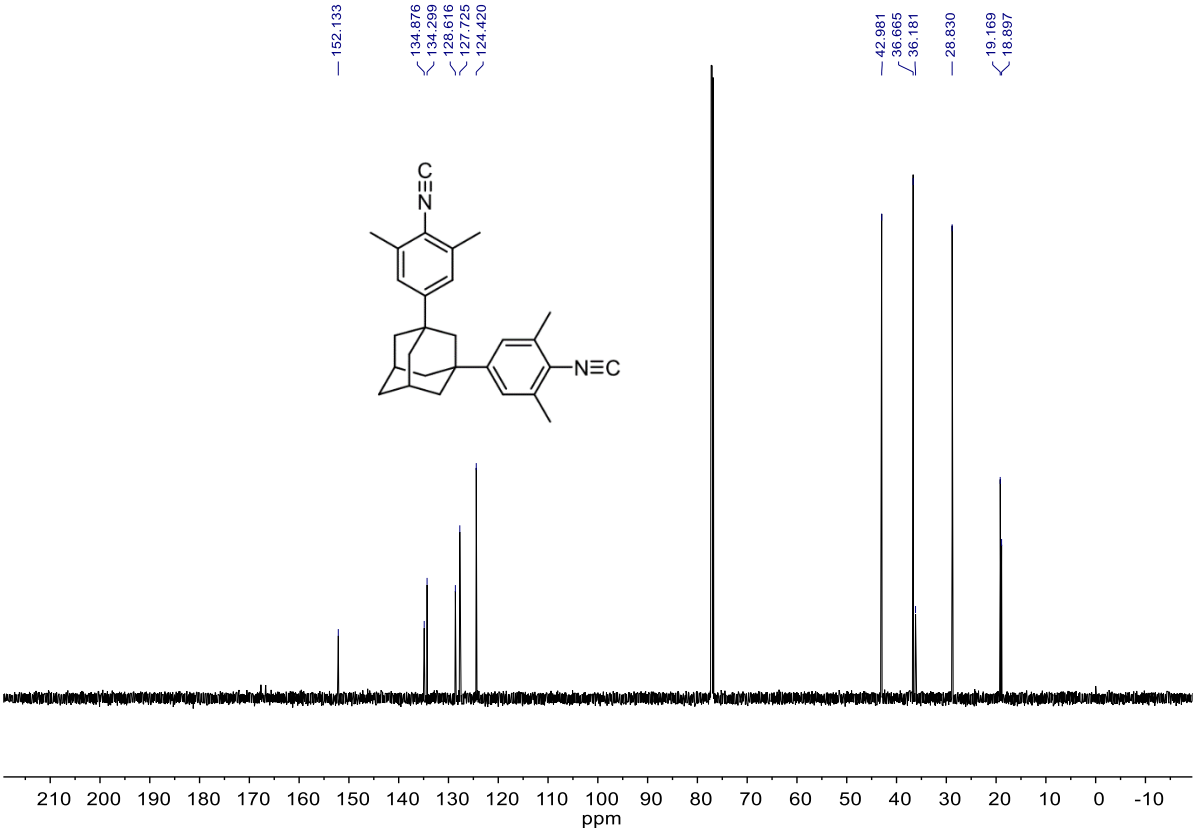

Figure S18. ^{13}C NMR spectrum of **Ad2** in $CDCl_3$.

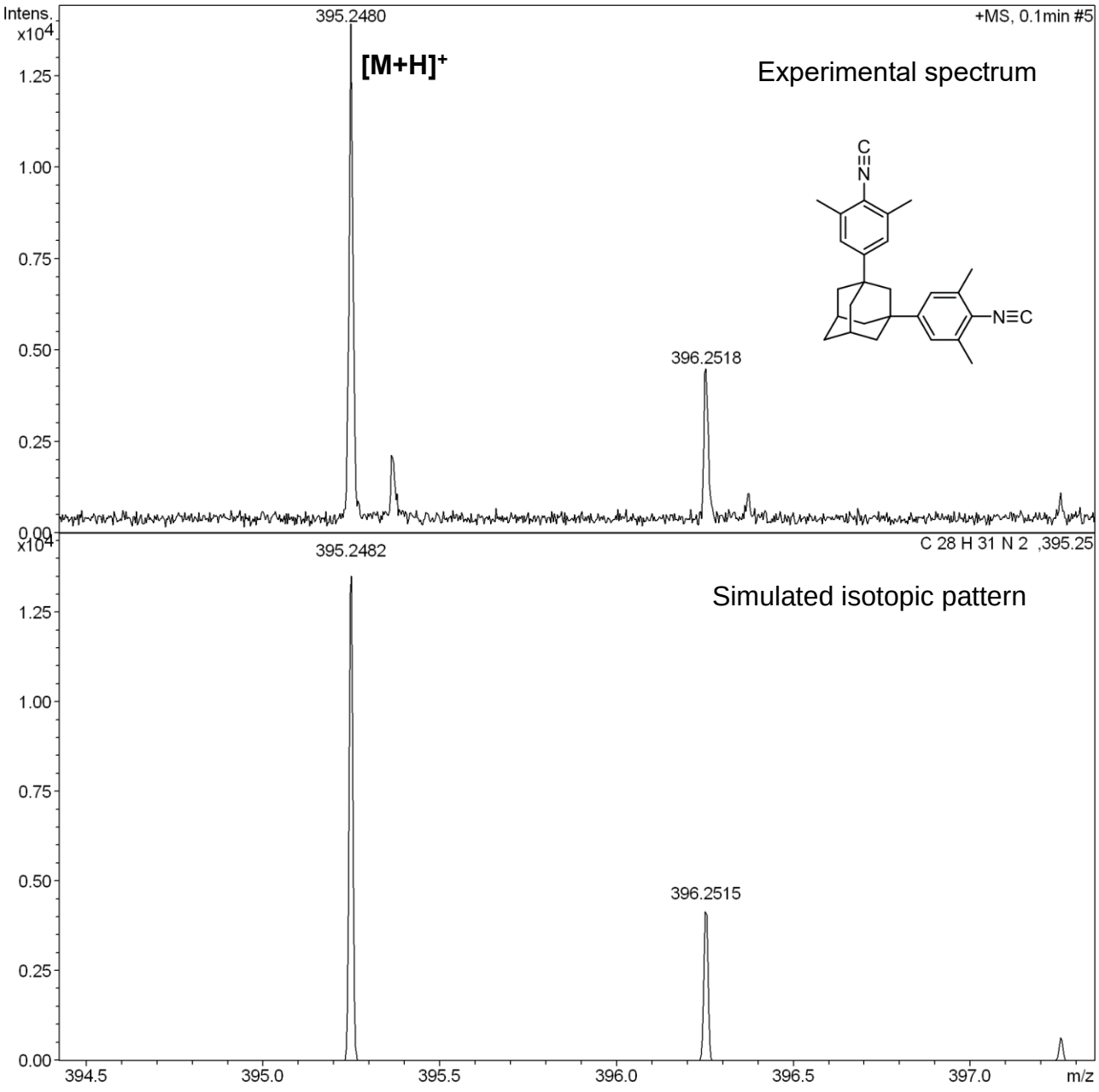

Figure S19. Mass spectrum of **Ad2**.

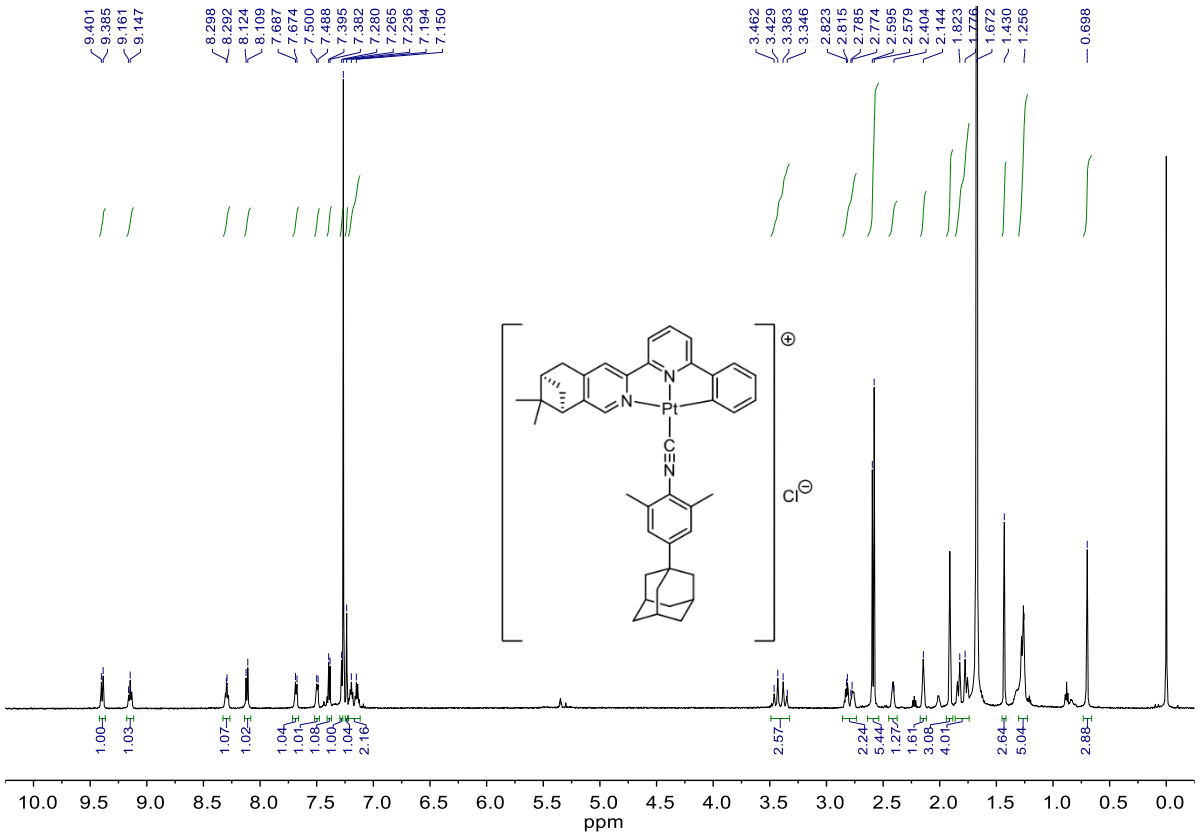

Figure S20. ^{1}H NMR spectrum of **Pt-1(Cl)** in $CDCl_3$.

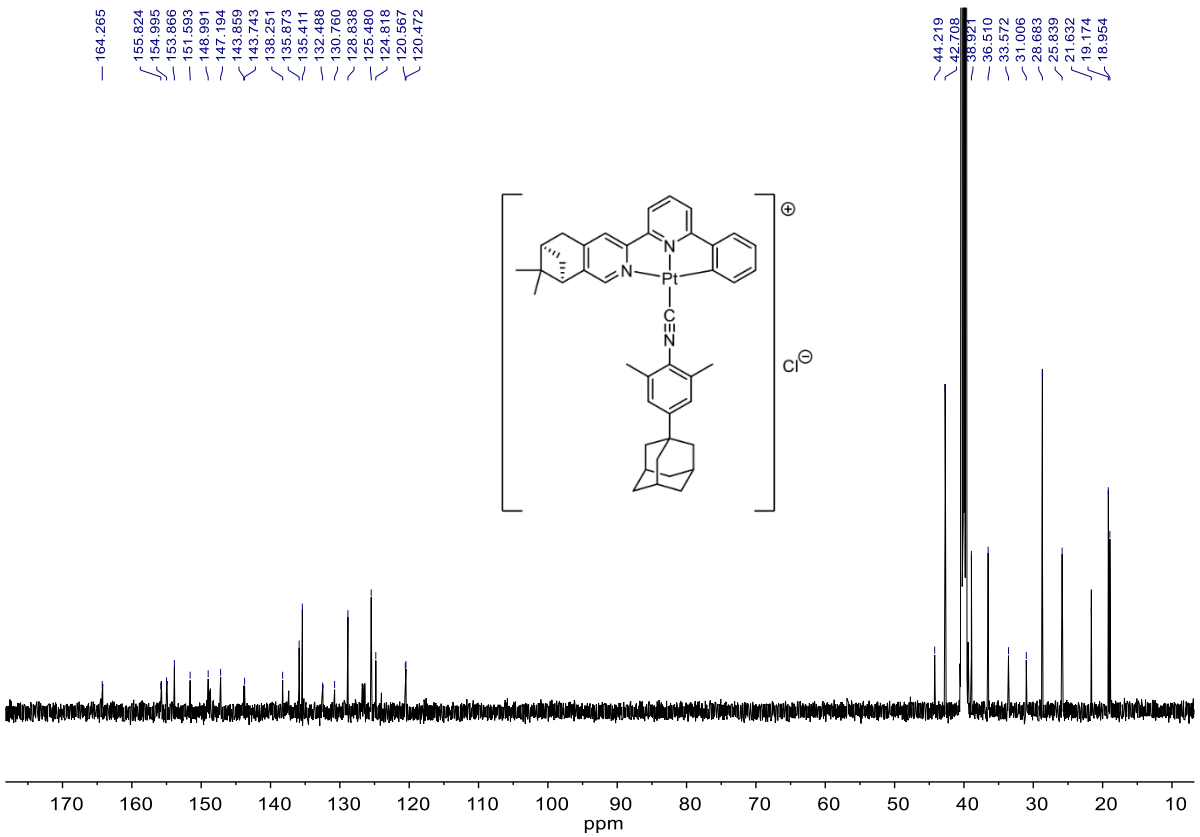

Figure S21. ^{13}C NMR spectrum of **Pt-1(Cl)** in $CDCl_3$.

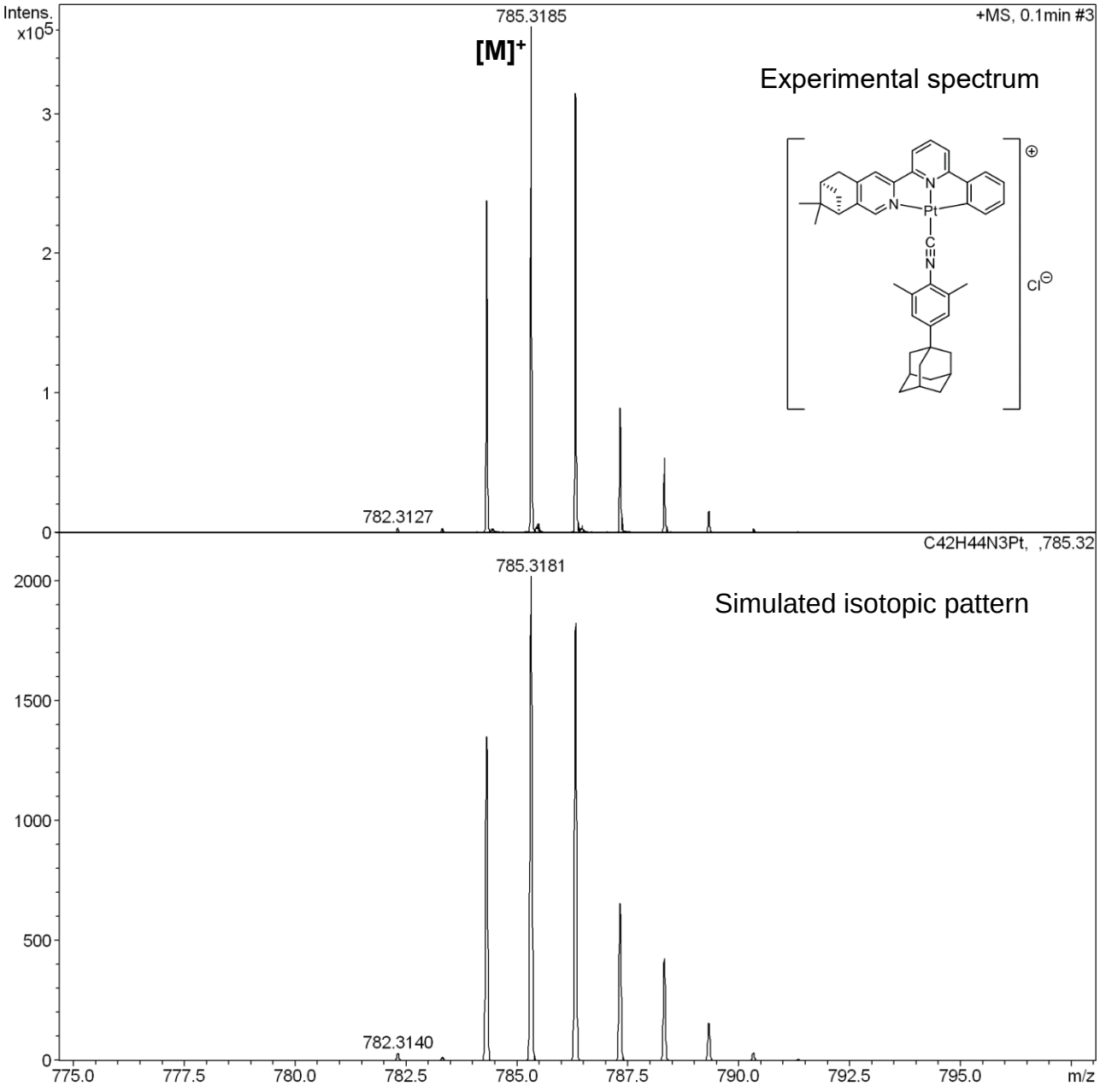

Figure S22. Mass spectrum of **Pt-1(Cl)**.

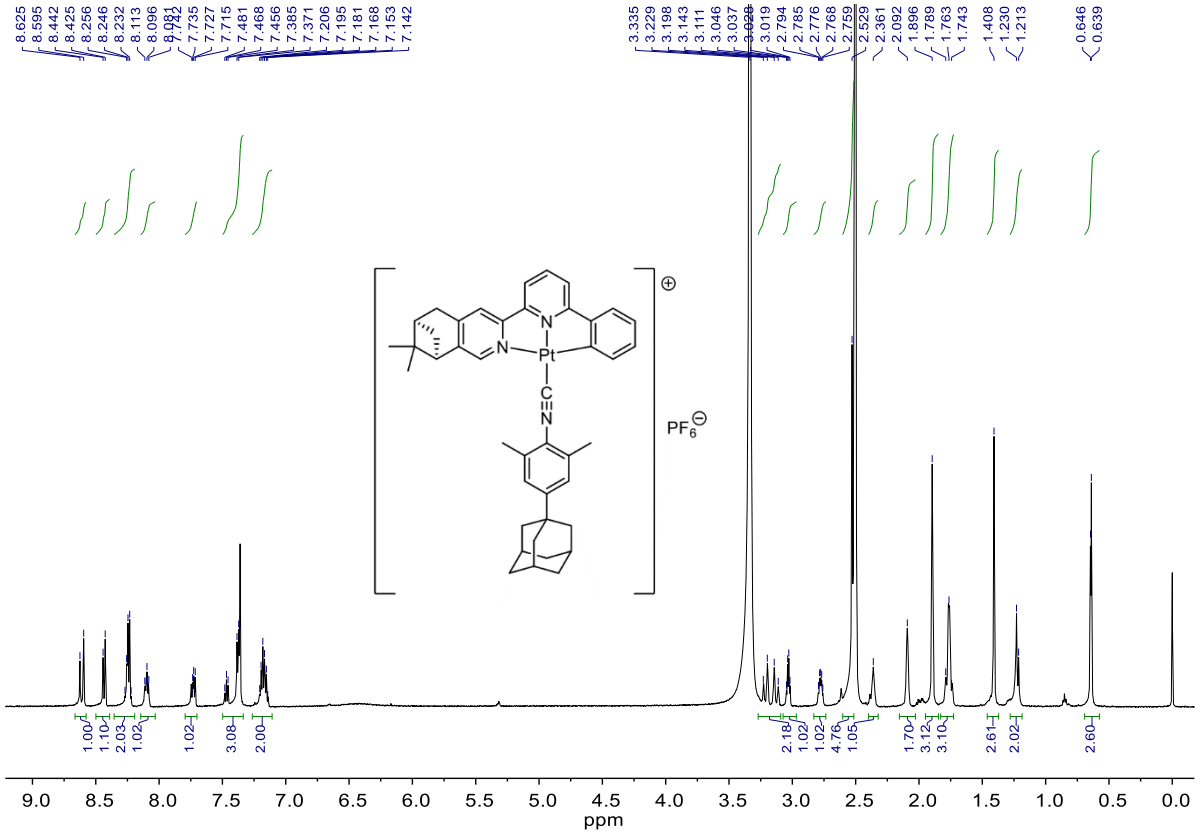

Figure S23. ^{1}H NMR spectrum of **Pt-1(PF$_6$)** in d6-DMSO.

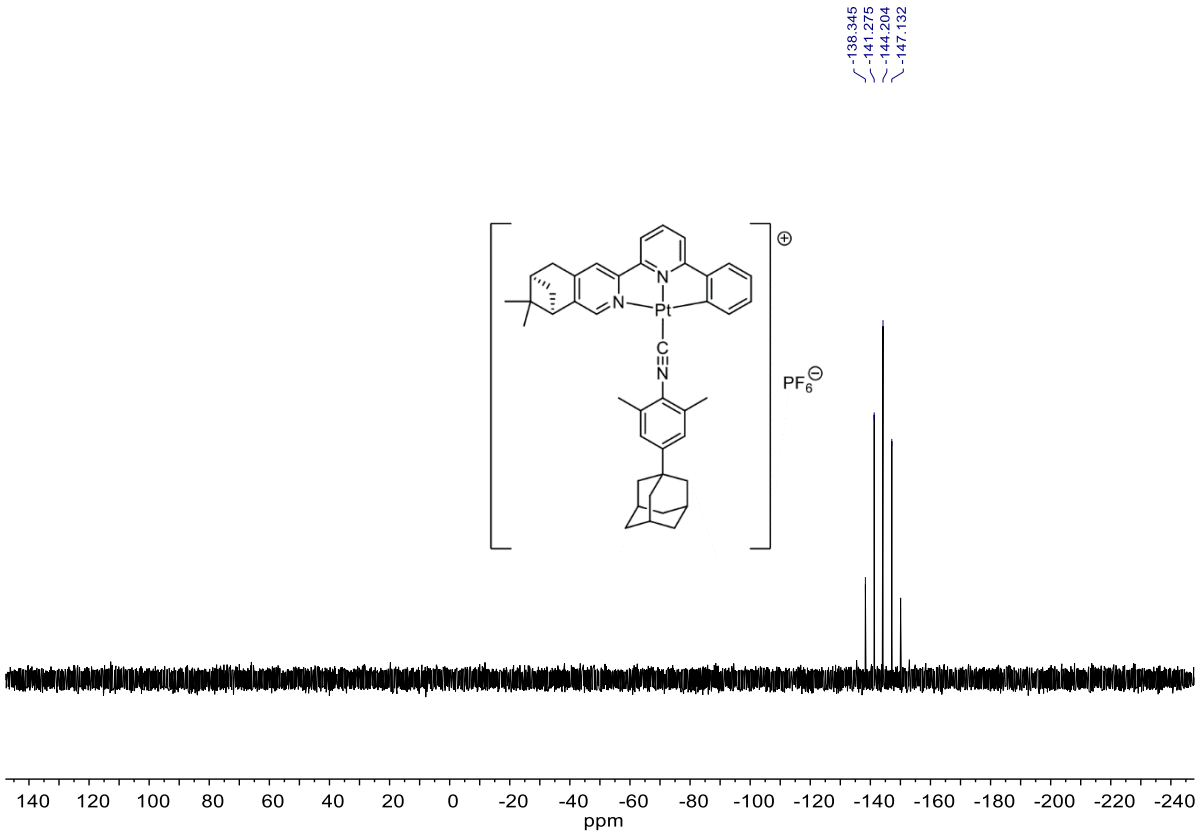

Figure S24. ^{31}P NMR spectrum of **Pt-1(PF$_6$)** in d6-DMSO.

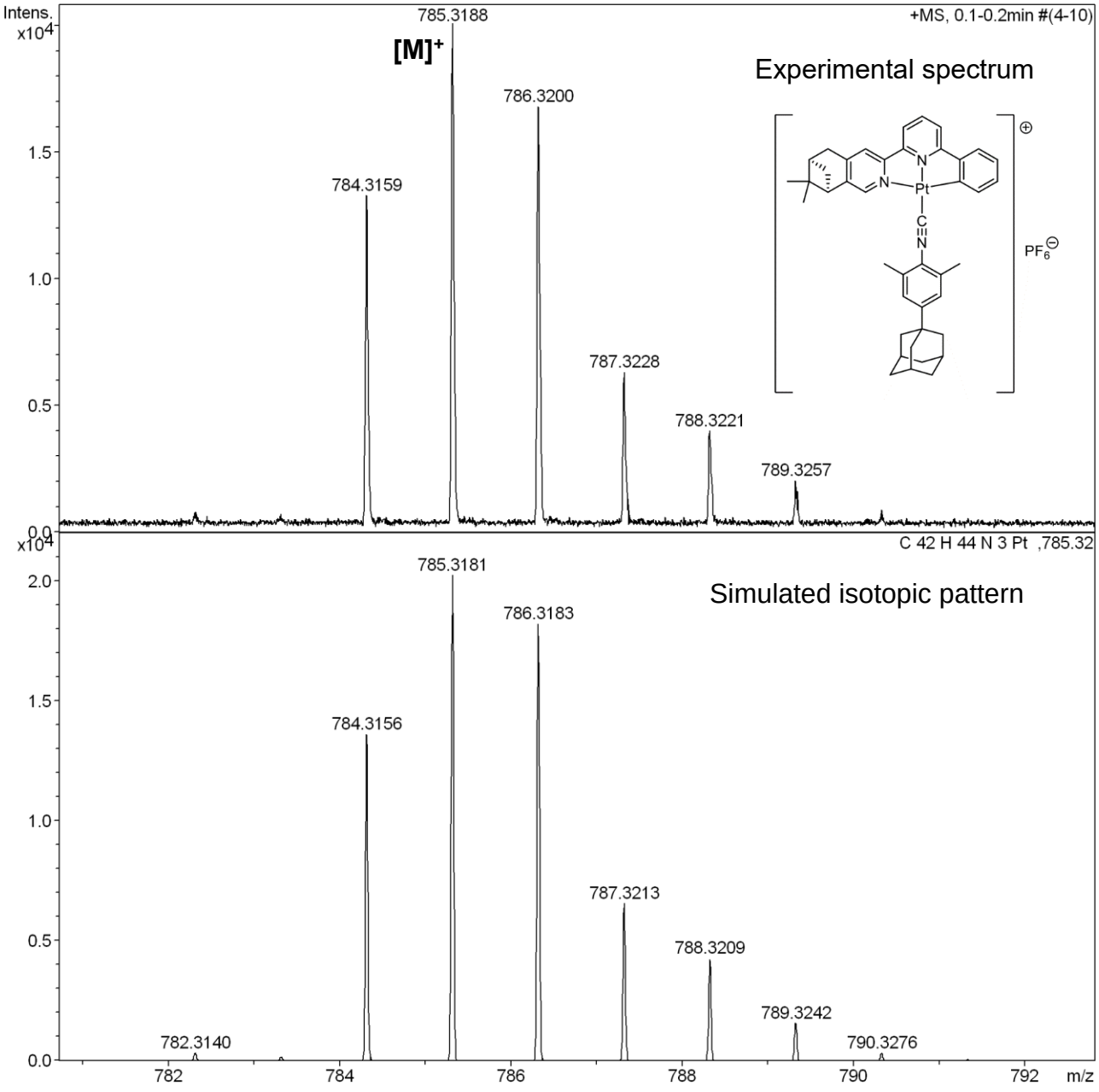

Figure S25. Mass spectrum of **Pt-1(PF_6)**.

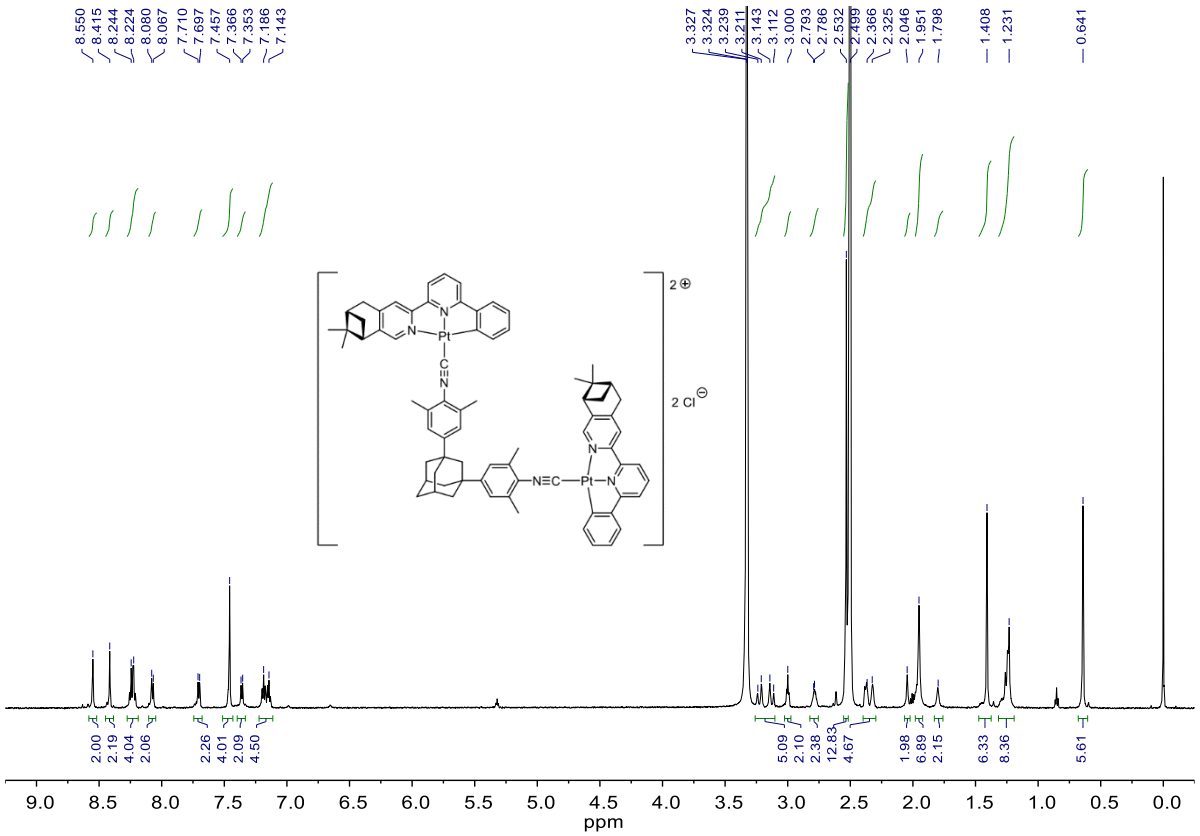

Figure S26. ^{1}H NMR spectrum of **Pt-2(Cl)$_2$** in d6-DMSO.

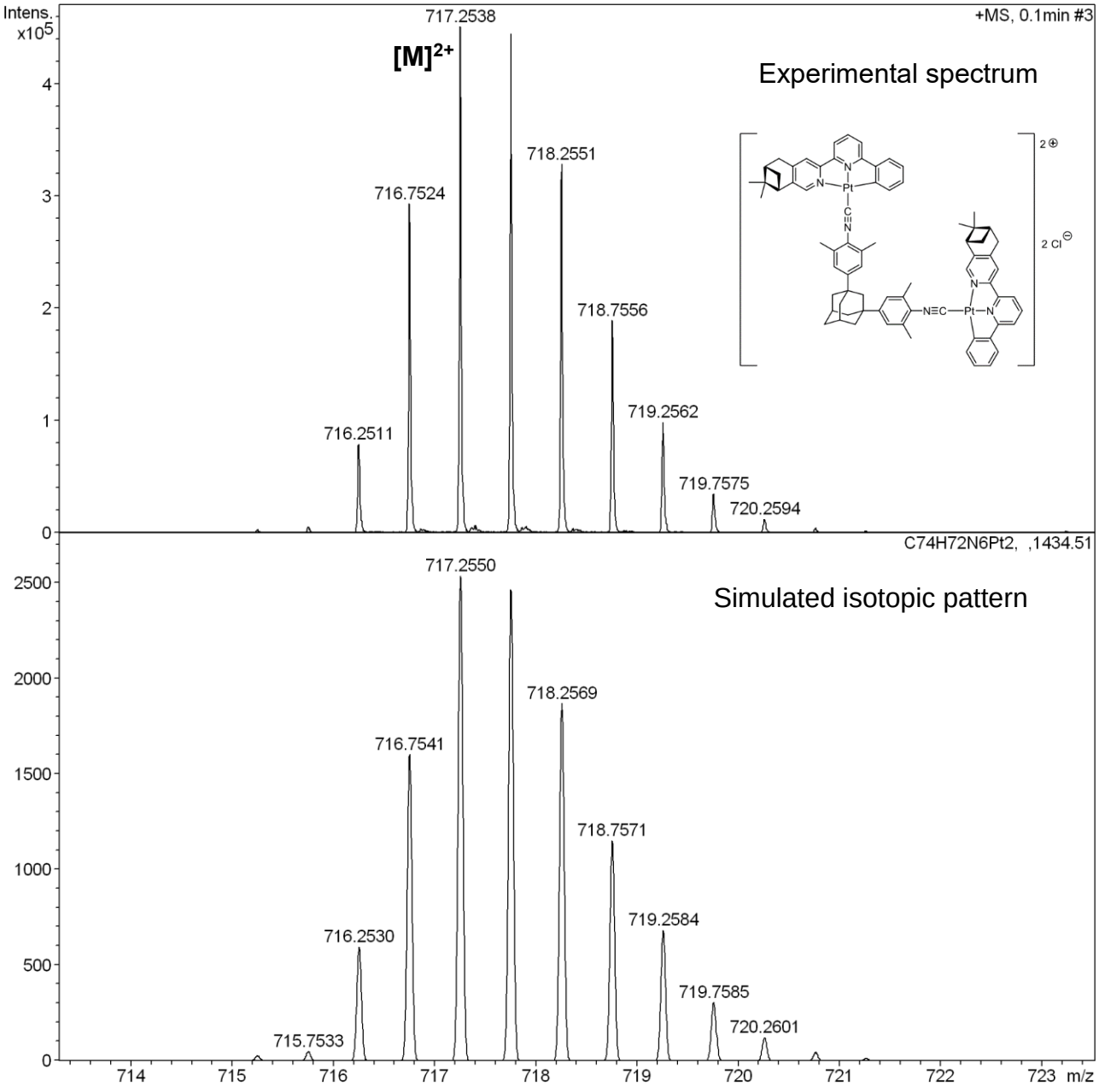

Figure S27. Mass spectrum of **Pt-2(Cl)$_2$**.

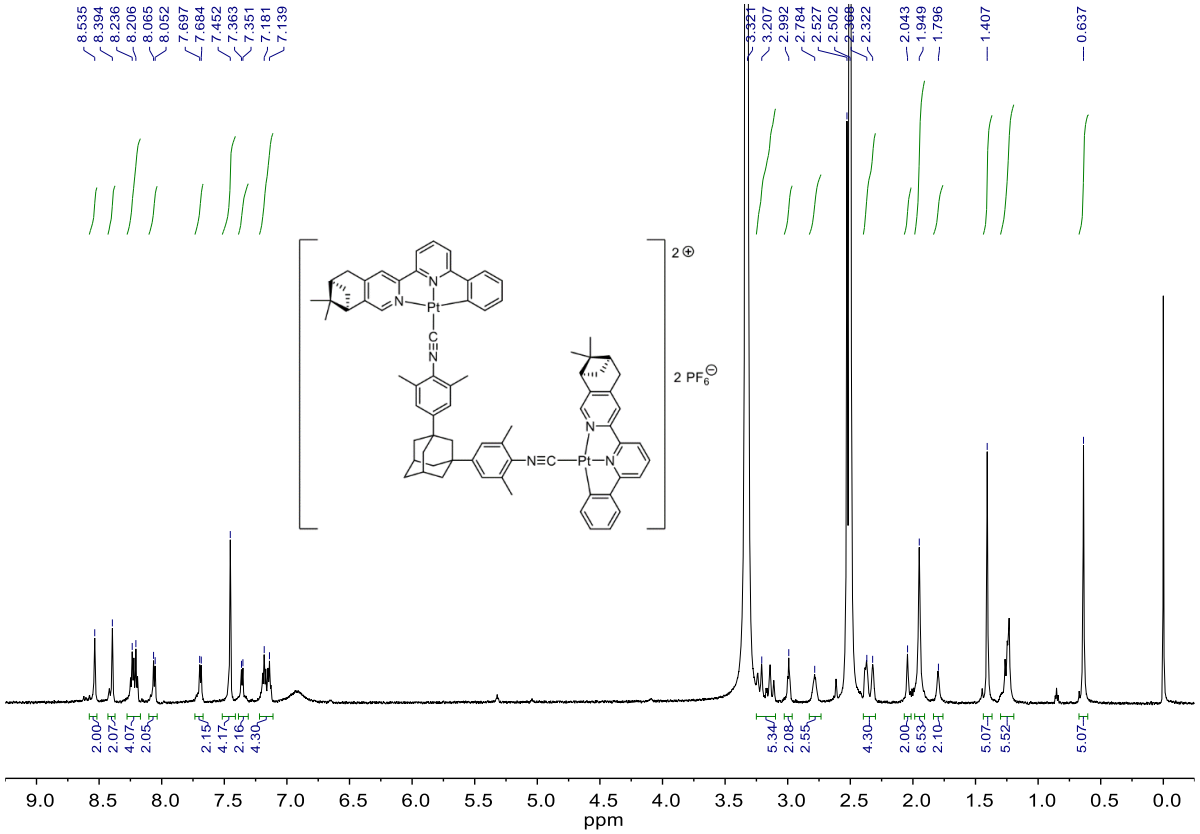

Figure S28. ^{1}H NMR spectrum of **Pt-2(PF$_6$)$_2$** in d6-DMSO.

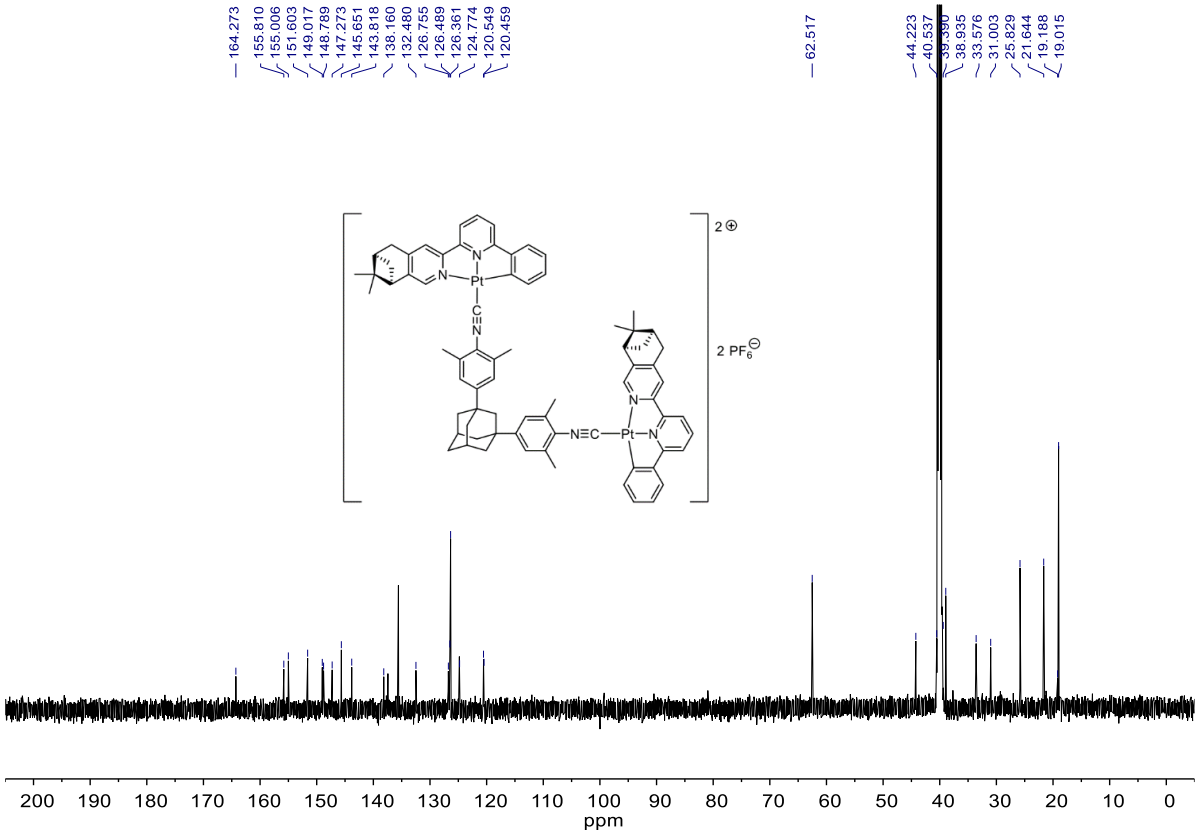

Figure S29. ^{13}C NMR spectrum of **Pt-2(PF$_6$)$_2$** in d6-DMSO.

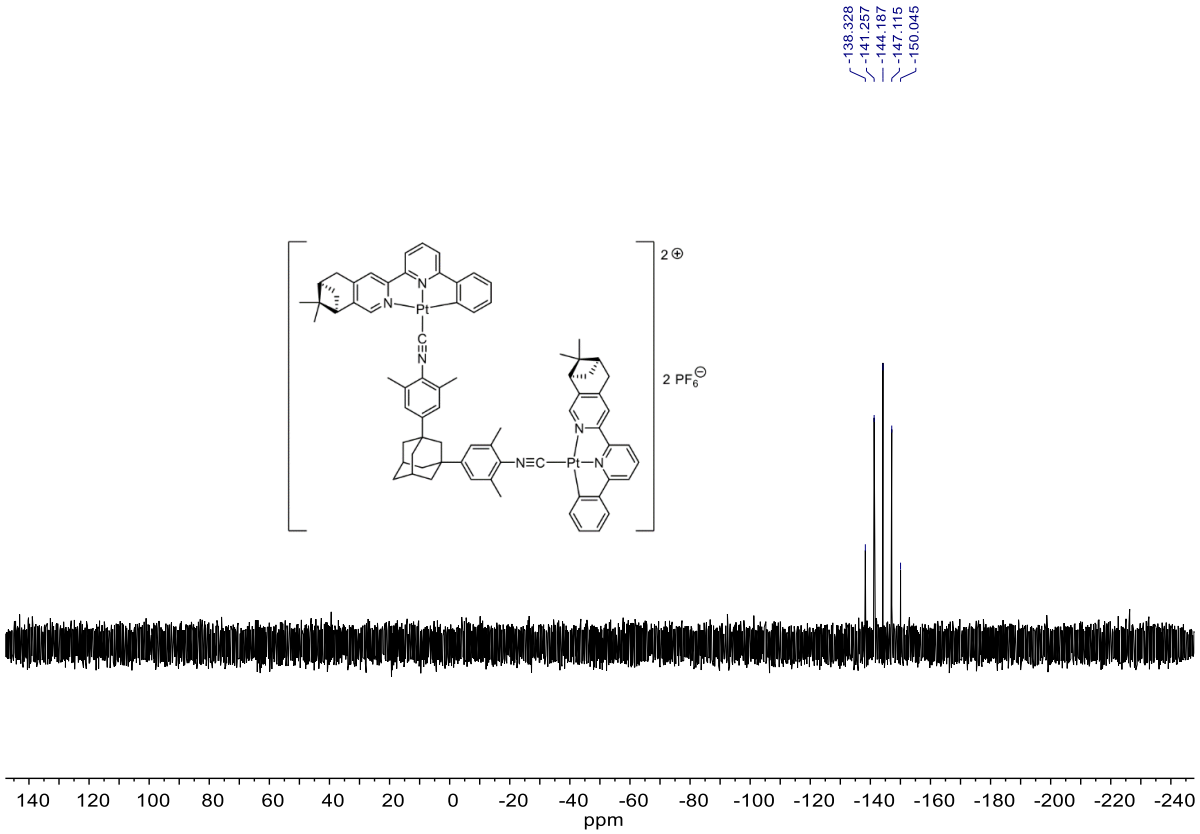

Figure S30. ^{31}P NMR spectrum of **Pt-2(PF$_6$)$_2$** in d6-DMSO.

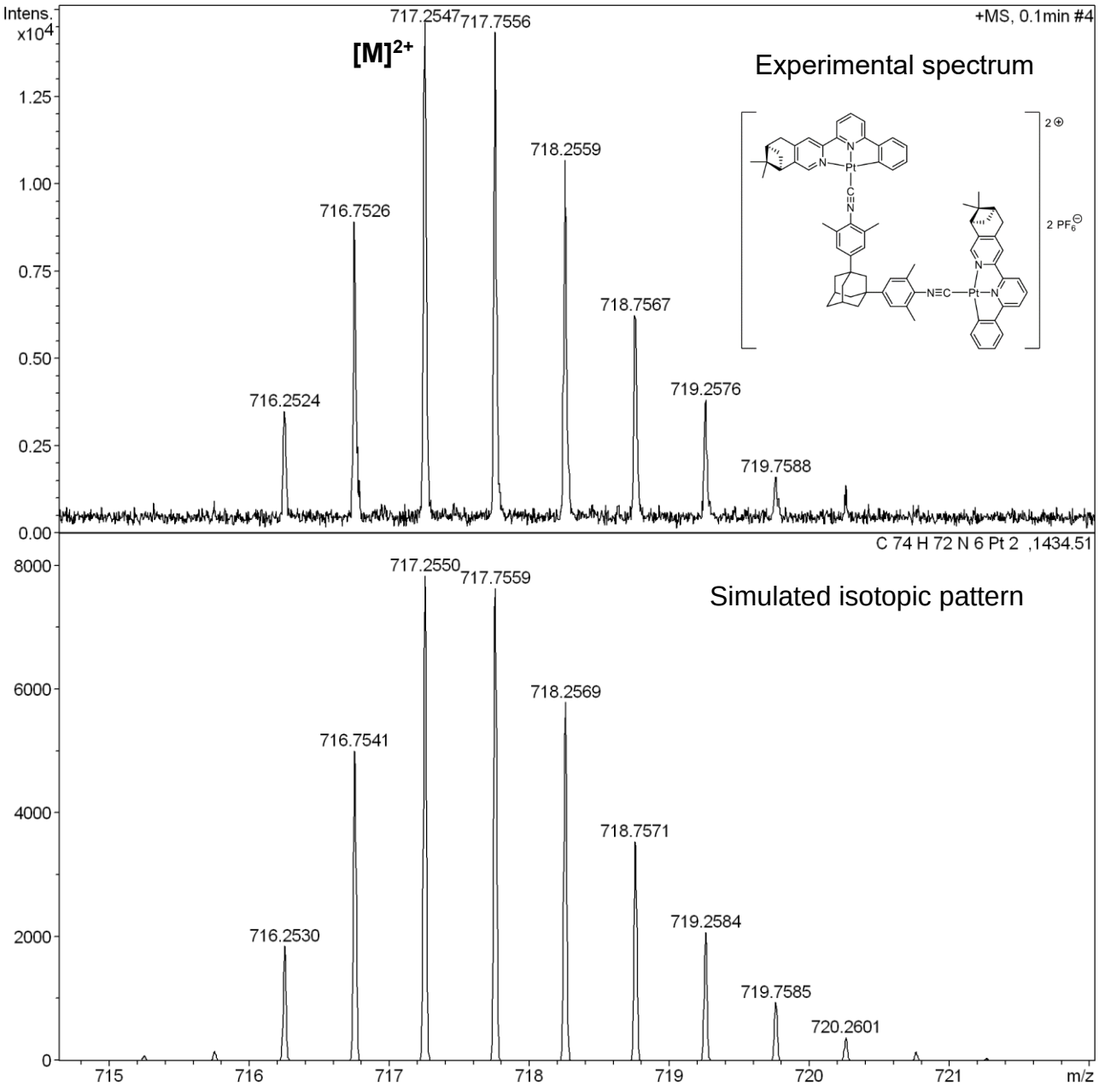

Figure S31. Mass spectrum of **Pt-2(PF$_6$)$_2$**.

References

[S1] Zhang, X.-P.; Wu, T.; Liu, J.; Zhang, J.-X.; Li, C.-H.; You, X.-Z. Vapor-induced chiroptical switching in chiral cyclometalated platinum(ii) complexes with pinene functionalized C^N^N ligands. *J. Mater. Chem. C* **2014**, *2*, 184-194.